Quantifying Isopycnal Heave Using Dynamic Depth Warping

A Thesis Presented

by

Maya V. Chung

to

The Department of Earth and Planetary Sciences

in partial fulfillment of the requirements

for a degree with honors of Bachelor of Arts

April 2019

Harvard College

Abstract

Changes in the depth of isopycnals are an important indicator of ocean circulation variability, and changes in the thickness of oceanic layers between these isopycnals affect the ocean inventory of heat and carbon. The conventional use of potential density to calculate isopycnal heave and layer thickness can mask much of the variability present in independent temperature and salinity measurements. We present a novel application of dynamic warping to vertical temperature and salinity profiles by simultaneously computing their optimal distance to time-averaged profiles, thus quantifying isopycnal heave throughout the water column. Synthetic tests show this warping method outperforms the conventional density-based method in low stratification and noisy data, implying the versatility of the novel warping method to calculate heave consistently in a global ocean dataset.

We first apply this technique to station data from the Hawaii Ocean Timeseries and the Bermuda Atlantic Time-series Study, yielding heave estimates at monthly resolution over the past 30 years through the full depth of the ocean. Next, we calculate heave in Argo float profiles of the upper 2000 m of the ocean within 50 km of the Hawaii station, and demonstrate correspondence in heave estimates between these independent datasets. We then calculate heave in all the Argo data in the North Pacific Ocean, and use a linear model to measure the contributions of seasonal variability, the El Niño-Southern Oscillation, and decadal heaving trends to heave in the North Pacific. Seasonal variability and ENSO dominate in the equatorial regions, while warming trends dominate at high latitudes. We also find coherent heave patterns in the deep Equatorial Pacific and long-term shifts in the position of the Kuroshio Current. Finally, we calculate the total heat uptake in the upper 2000m of the high-latitude North Pacific to be 0.88 W m^{-2}. Future work will investigate the ability of the global Argo array to constrain long-term heaving trends associated with ocean heat uptake, in an ocean rich with internal-wave and mesoscale-eddy variability.

Contents

List of Figures

Acknowledgements

This work would not have been possible without the contributions and support of several people. Firstly, I want to extend my utmost gratitude to Peter Huybers for being a wonderful thesis advisor and my academic advisor in Earth and Planetary Sciences for the past three years. His input and feedback were critical for this work, and I appreciate his willingness to both challenge and encourage me to become a better scientist. Next, I want to thank Jake Gebbie from Woods Hole Oceanographic Institution for contributing his valuable perspective to this work and for being a fantastic and supportive mentor during Summer 2018. I also want to thank my mentors from Scripps Institution of Oceanography, Ivana Cerovecki, Matthew Mazloff, Sarah Gille, and Lynne Talley, for giving me a foundation in physical oceanography research and for their continued support. Thank you also to the many scientists who provided important feedback on this work, especially Rui Xin Huang, Breck Owens, and David Nieves.

I must also thank the Harvard EPS Department for being such an integral part of this work and my college experience. Thank you to the thesis preceptors, Esther James and Annika Quick, for their valuable guidance and support. Thank you to my Women-in-STEM mentors, Judy Pu and Rachel Silvern. Thank you to the Huybers group for sharing their wisdom and being amazing role models. Thank you to Sabinna Cappo for her positivity and encouragement. Finally, I owe everything to Chenoweth Moffat, who convinced me to concentrate in EPS and continually inspires me with her enthusiasm.

This work would not have been possible without the support of my peers. Thank you to the other EPS thesis writers, Becca Cleveland-Stout, Molly Wieringa, Maggie Powell, and Thomas Lee. Their support when I needed it most was truly what got me through this thesis. Thank you especially to Thomas for being my "accountability buddy" this year, and being there for me ever since the first day of geology class. I cannot think of a more amazing group of people to have shared this experience with. Thank you also to the 2018 WHOI Summer Student Fellows for inspiring me every day with their passion for understanding the Earth.

This work was also supported by the Woods Hole Oceanographic Institution Summer Student Fellowship, which funded my research for 12 weeks during Summer 2018, and an AGU Student Travel Grant.

Lastly, thank you to my family for supporting my dream of becoming an oceanographer. Mom, thank

you for teaching me the meaning of this work, and that the actions of one person can make a big difference. Dad, thank you for giving me your old oceanography textbooks and for constantly challenging my ideas. Nina, thank you for inspiring me every day with your talent and passion. This thesis is dedicated to all of you.

Chapter 1

Introduction

Predicting the consequences of anthropogenic climate change requires understanding the ocean. Since 1971, 93% of the excess heat associated with anthropogenic emissions of greenhouse gases has been absorbed by the ocean (*Church et al.*, 2011). Although the ocean has slowed the rate of global surface warming by absorbing heat and carbon, this absorption also influences large-scale weather patterns, sea level rise, and ocean acidification; thus the heat content of the ocean is of major concern. For decades, oceanographers have studied ocean heat uptake and other phenomena by measuring changes along *isopycnals*, or surfaces connecting water with the same density. Isopycnals are influenced by several processes related to both climatic trends and natural variability, and distinguishing between the two can be difficult. The vertical movement of isopycnals, or *heave*, can be influenced by ocean warming as well as changes in winds and ocean circulation. Quantifying the influence of isopycnal heave on ocean measurements can help characterize ocean variability on monthly to multidecadal timescales.

However, despite the expectation that heave is present throughout the world oceans, heave is not well-constrained everywhere. Additionally, conventional methods for measuring isopycnal heave are likely to mischaracterize heave because they rely on potential density, which can mask changes in temperature and salinity. We wondered whether we could improve upon conventional methods for measuring heave by creating a new technique that incorporates temperature and salinity measurements independently. We could then apply our technique to global ocean data to better quantify heave and the ocean processes associated with heave throughout the world oceans.

1.1 Ocean Heat Content and Climate Sensitivity

Perhaps the most elusive number in climate science is the Earth's temperature response to a change in radiative forcing, or climate sensitivity. This number is most often expressed as the Earth's temperature change after reaching an equilibrium state in response to a doubling of atmospheric CO_2. Climate sensitivity is influenced by major feedbacks in the climate system, including ocean heat uptake. The ocean's heat capacity is over 1000 times larger than that of the atmosphere, and the ocean can remove heat and carbon from the atmosphere and store it for hundreds to thousands of years (*Schmitt*, 2018). Ocean heat uptake's role as a stabilizing climate feedback is thus important for understanding the climate system and predicting future climate change.

Ocean heat content in both the upper and deep ocean is influenced by processes at the Earth's surface. Enhanced radiative forcing and increased surface temperatures increase upper ocean heat content through air-sea exchanges and wind-driven mixing (*Desbruyères et al.*, 2017). Indeed, the upper ocean (0-700m) has experienced the largest amount of heat uptake compared to the rest of the ocean, atmosphere, land, and cryosphere since 1971 (Fig. 1.1). Ocean heat uptake also varies geographically and with depth. This is due to the spatial variability of winds and water mass formation, which influence the subduction of water from the surface ocean to the interior ocean. Several studies have shown large heat uptake in the Southern Ocean, and increasing rates of warming in the deep Southern Ocean due to changes in Antarctic Bottom Water formation (*Purkey and Johnson*, 2010; *Häkkinen et al.*, 2016; *Desbruyères et al.*, 2017). There is also evidence that these changes extend to regions fed by Antarctic Bottom Water, such as the south Pacific and Atlantic (*Desbruyères et al.*, 2016). It has also been shown that the Southern Hemisphere is responsible for the majority of global ocean heat uptake, due to its large ocean volume and strong air-sea exchange in the turbulent Southern Ocean (*Desbruyères et al.*, 2017).

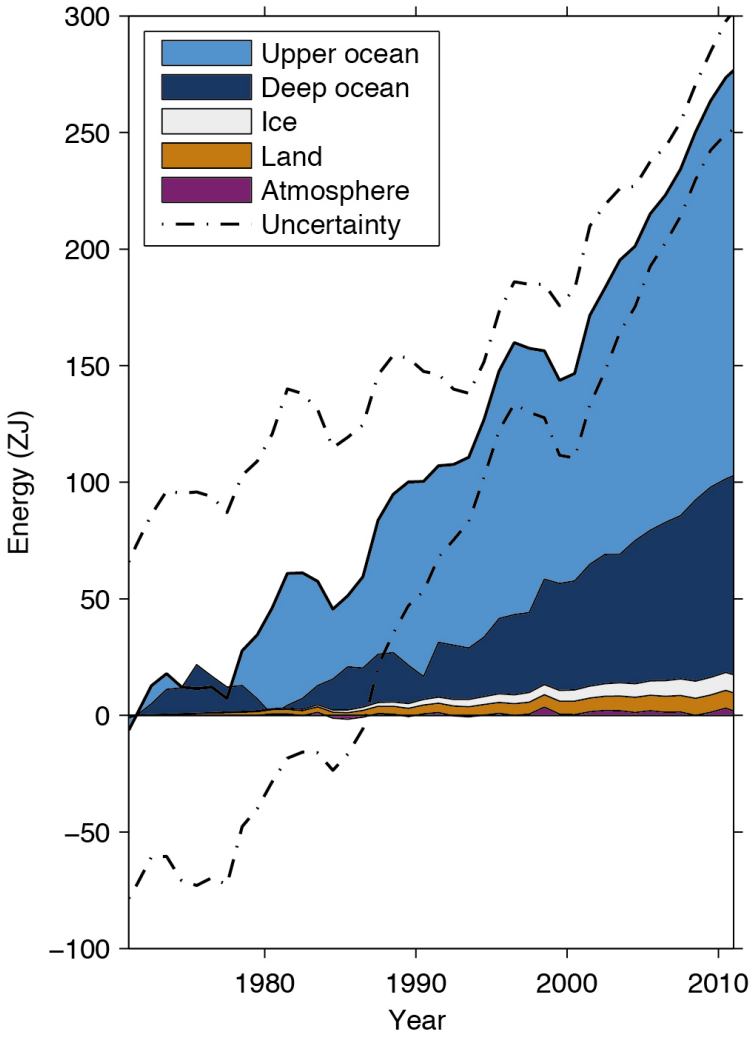

Figure 1.1: Ocean heat content since 1971 compared to ice, land and the atmosphere. "Upper ocean" is 0-700m depth, and "Deep ocean" is below 700m depth. Heat content is measured in Zetta-Joules (ZJ), or 10^{21} Joules. Dot-dashed lines indicate uncertainty at the 90% confidence interval for all components. From the 2013 Intergovernmental Panel on Climate Change Report (*Rhein et al.*, 2013).

There is still much uncertainty in ocean heat uptake estimates due to sparse data coverage. Oceanographers use vertical profiles of temperature, salinity, and depth to study changes in the ocean. When these profiles are collected in similar locations over time, this is referred to as repeat hydrography. There are very few locations in the ocean with regularly sampled repeat hydrography, presenting a challenge for resolving

high-frequency processes that influence ocean heat uptake. Deep ocean heat content is especially uncertain due to the difficulty of sampling the deep ocean, yet the deep ocean plays a large role in the overall estimate of ocean heat content. Models of ocean heat uptake have shown the importance of regularly monitoring ocean heat uptake down to 4000m depth (*Palmer et al.*, 2011), and the deep ocean (below 2000m) is expected to play a more prominent role in sequestering heat in the future (*Purkey and Johnson*, 2010). An extensive deep-ocean monitoring program is still in the works (*Jayne et al.*, 2017).

However, an existing dataset called Argo has the potential to improve our understanding of ocean heat uptake. With its unprecedented level of spatial and temporal coverage, it has the potential to resolve the high-frequency processes associated with surface and deep-ocean heat uptake.

1.2 Argo: A Revolution in Ocean Observation

Argo floats are autonomous floats that adjust their buoyancy to travel up and down in the ocean and measure attributes such as temperature, salinity, pressure, and velocity (*Jayne et al.*, 2017). These data are collected using CTDs, instruments that measure **C**onductivity, **T**emperature, and **D**epth. Argo floats record ocean profiles every 10 days; they drift at 1000m depth for 9 days, then descend to 2000m and rise to the surface to record a 2000m profile. When the floats reach the surface, they transmit their data to a satellite and record their location using GPS, then restart the cycle. The floats repeat this process until they run out of battery after about 5 years (*Jayne et al.*, 2017). With the support of an international coalition of government agencies, the first Argo floats were deployed in 1999 (*Roemmich et al.*, 2009). In 2007, the Argo program reached their goal of 3000 active floats, and today there are over 4000 active floats all over the global ocean (Fig. 1.2) (*Roemmich et al.*, 2009; *Argo*, 2000).

The Argo program was revolutionary in several ways. Before Argo, ocean measurements were primarily ship-based, and therefore very costly (*Durack et al.*, 2018). The autonomous nature of the floats reduced the cost of ocean observation from over $10,000 down to $200 per profile (*Jayne et al.*, 2017). The data is also freely available in near-real time, making timely oceanography research possible without going to sea (*Roemmich et al.*, 2009). Additionally, as an internationally-supported program from the start, the Argo program is one of the largest and most successful feats of international cooperation in all of oceanography

(*Jayne et al.*, 2017).

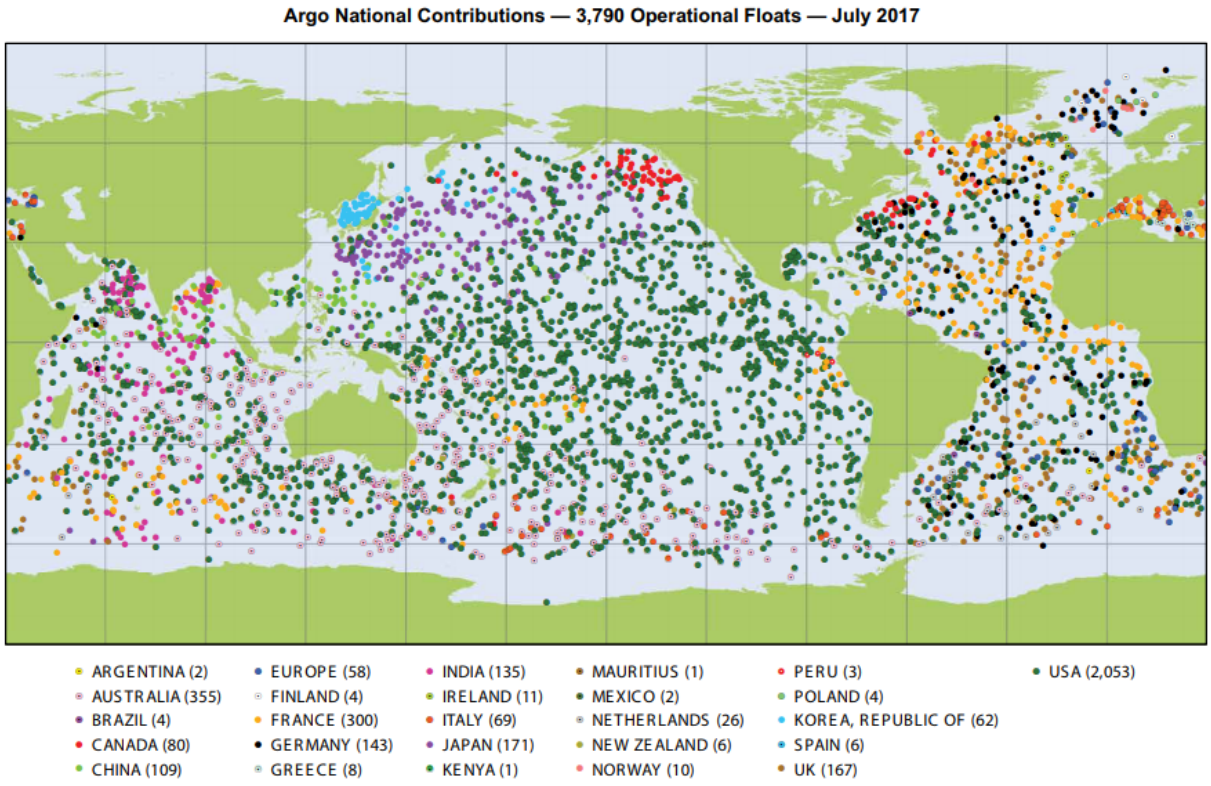

Figure 1.2: Locations of Argo floats in July 2017, with contributions to the Argo program by nation. From (*Jayne et al.*, 2017).

Argo completely changed our understanding of the ocean by providing unprecedented spatial and temporal sampling of the interior ocean. Before the late 1990s, ocean observation was so sparse that estimates of global sea surface temperature changed depending on what sampling method was used to collect the data (*Rhein et al.*, 2013). Argo has collected over 1.8 million ocean profiles, more than doubling the number of available ocean observations (Fig. 1.3) (*Durack et al.*, 2018; *Jayne et al.*, 2017). Data coverage increased the most in the Southern Hemisphere (Fig. 1.3), which was useful for constraining global ocean heat content because the Southern Hemisphere absorbs more heat than the Northern Hemisphere (*Desbruyères et al.*, 2017). Argo float data in the Southern Ocean illuminated the Southern Ocean's prominent role in ocean heat uptake and ocean circulation (*Roemmich et al.*, 2009; *Gille*, 2008).

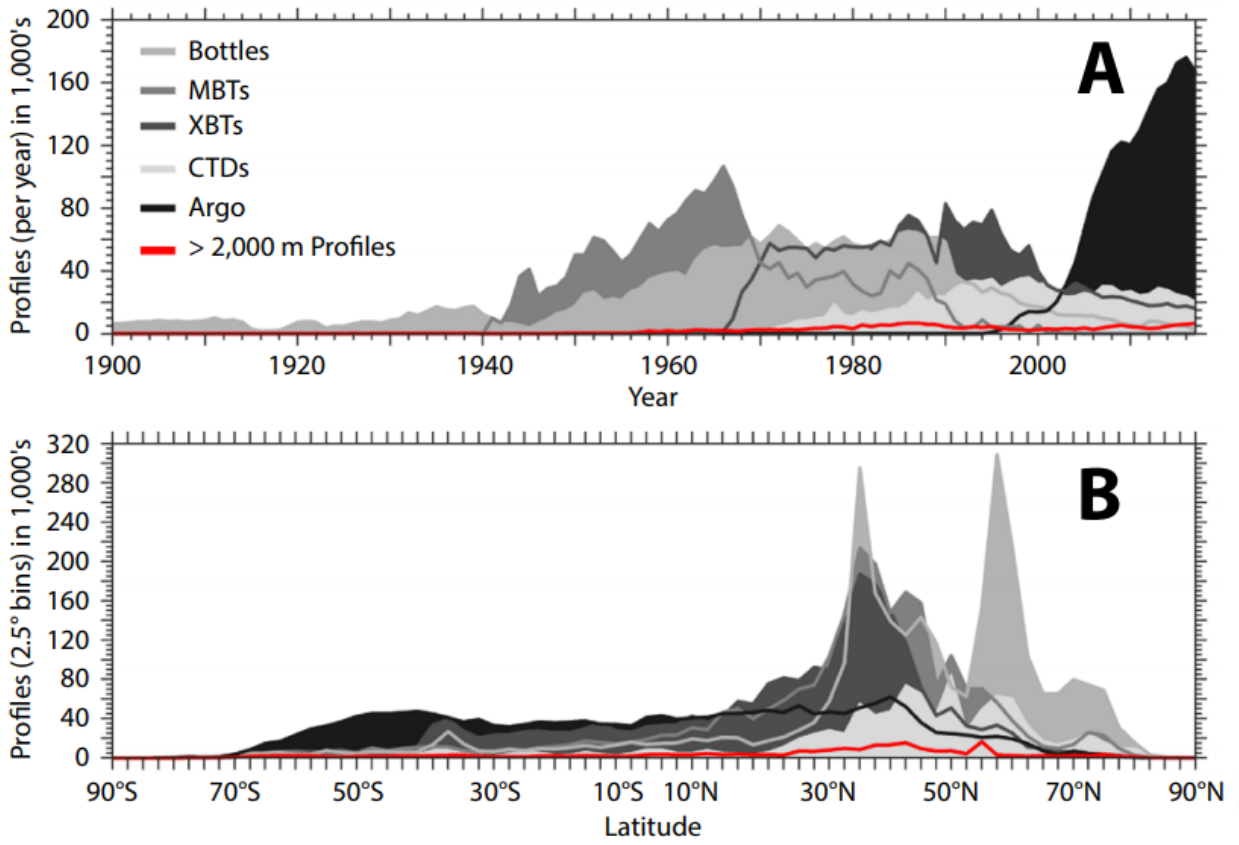

Figure 1.3: (A) Contributions to ocean observational data since 1900 by collection method, including ship-based methods (Bottles, mechanical bathythermographs, expendable bathythermographs, CTDs) and Argo floats (black). (B) The latitudinal distribution of measurements by collection method. Red lines indicate the amount of profiles collected per year in thousands exceeding 2000m depth. From *Durack et al.* (2018).

Argo floats also allowed oceanographers to examine large-scale changes in the interior ocean, such as El Niño and the movement of water masses, which complimented satellite measurements of sea surface height and sea level rise (*Nerem et al.*, 1997; *Roemmich et al.*, 2009). The Argo program prompted a large leap forward in constraining ocean heat content and understanding the ocean's role in the climate system.

After nearly a decade of global Argo measurements, oceanographers were able to quantify ocean heat content down to 2000m depth across the globe. The Argo data show evidence of global interior ocean warming (Fig. 1.4) (*Wijffels et al.*, 2016; *Roemmich et al.*, 2015). The globally-averaged upper ocean experienced the most warming but also had the highest variability due to its proximity to the surface. In contrast, the

intermediate depths (500-2000m) experienced steady warming of 0.002 °C/yr (*Roemmich et al.*, 2015).

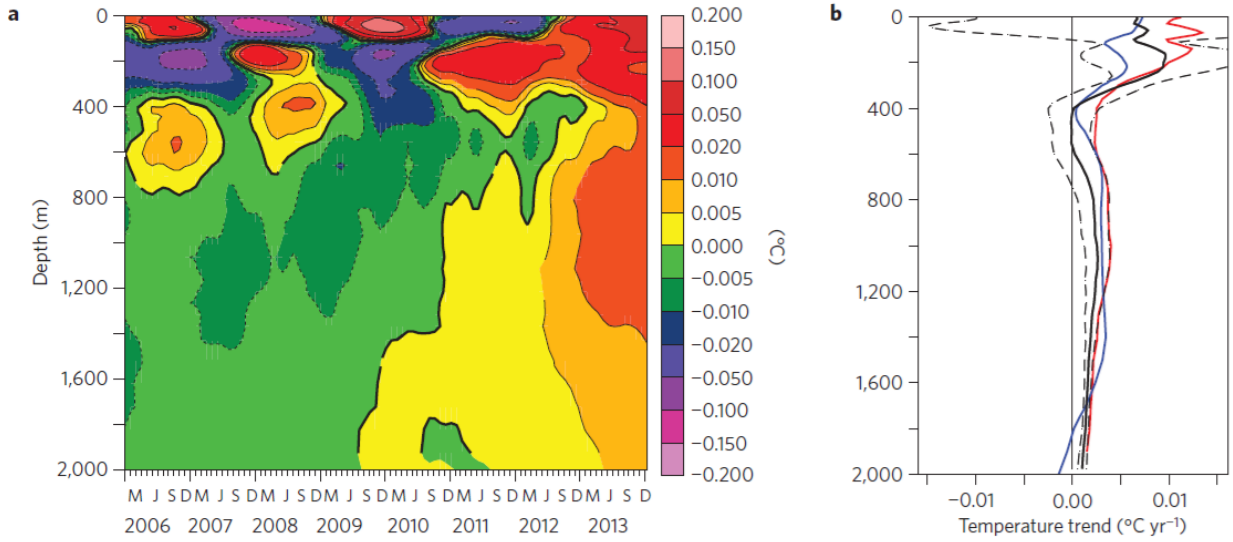

Figure 1.4: (a) Globally-averaged temperature anomaly (°C) with depth, as detected by Argo from 2006-2013. (b) Global average temperature trend (°C/yr) with depth, from three different Argo interpolation methods (solid lines) with 95% confidence interval (dashed lines). From *Roemmich et al.* (2015).

However, these ocean heat content changes naturally have large spatial variability, because changes in ocean heat content are highly dependent on ocean dynamics (Fig. 1.5) (*Roemmich et al.*, 2015). These dynamics are indicative of the redistribution of heat content rather than long-term trends, and this effect can only be averaged out with global-scale averaging (*Roemmich et al.*, 2015). This demonstrates the importance of understanding the dynamical processes that influence ocean heat content. It would therefore be useful to find a way to use Argo data to study these ocean dynamics alongside long-term trends.

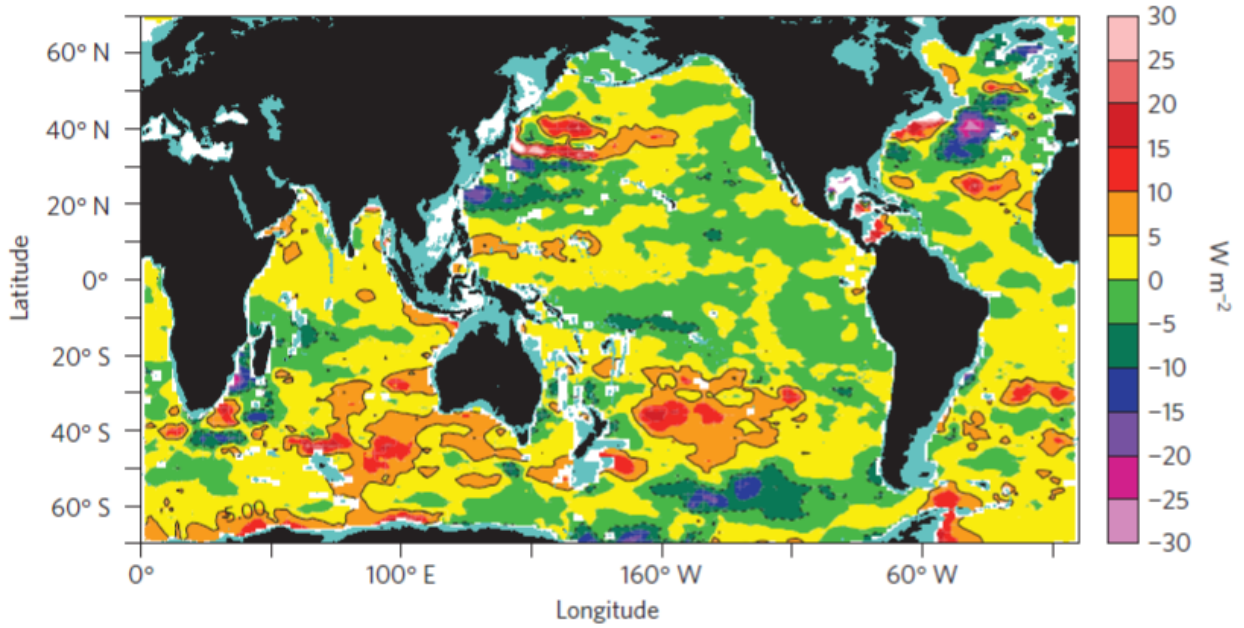

Figure 1.5: Ocean heat content trends as detected by Argo from 2006-2013, averaged from 0-2000m depth. Contours represent ± 5 W/m^2. Modified from *Roemmich et al.* (2015).

Despite the current Argo product only reaching 2000m, Argo still has considerable untapped potential to describe ocean dynamics and heat content. Deep-Argo floats that can take measurements down to 6000m depth are currently being tested and deployed (*Jayne et al.*, 2017). These new floats will be very useful, as it is estimated that this array could reduce the uncertainty of global ocean heat uptake by nearly six-fold (*Johnson et al.*, 2015). However, it will take many years to achieve global Deep-Argo coverage. The current Argo array has collected about a decade's worth of global ocean data, and the repeat hydrography provided by Argo is reaching the point where there is enough spatial and temporal coverage to study more high-frequency processes in the ocean (*Katsumata*, 2016). There are challenges to doing so because Argo floats do not represent fixed points of observation; rather, they are constantly moving and collecting data as dictated by ocean currents. However, if we successfully convert the Argo dataset to a format that describes ocean dynamics and wave propagation through the interior ocean, we could reach a new level of understanding of ocean variability and the ocean's role in the climate system.

1.3 Interpreting Ocean Data Using Isopycnal Heave

The large-scale mixing processes that affect ocean heat content tend to occur along neutral surfaces or *isopycnals*, surfaces of constant density (*McDougall*, 1984). It is useful to study the vertical motion of isopycnals, or *heave*, because heave is indicative of several types of oceanic processes. Heave is the dominant process associated with ocean heat uptake on interannual to decadal scales, especially in the upper ocean (*Bindoff and McDougall*, 1994). Heave can also be generated by high-frequency processes that occur naturally. Mesoscale eddies, swirling whirlpools that form by pinching off from currents, can cause heave through upwelling or downwelling and transporting water masses laterally across the ocean (*Katsumata*, 2016). The seasonal subduction of warm waters into the shallow ocean causes changes in the thermocline and gradual deepening of isopycnals (*Bindoff and McDougall*, 1994; *Johnson and Marshall*, 2002). Seasonal changes in Ekman pumping and water mass formation cause heave by changing the thickness of the layers between isopycnals (*Jayne and Marotzke*, 2001; *Kawase*, 1987; *Nieves and Spall*, 2018). Accurately quantifying heave is thus an important step in studying various natural and climatic ocean processes, and using the Argo dataset to quantify isopycnal heave on a global scale would provide new insight into ocean variability.

1.4 Previous Methods for Measuring Heave

1.4.1 Heave/Spice Decomposition

Bindoff and McDougall (1994) first proposed a framework for interpreting ocean data in three components: pure warming or cooling, pure freshening or salinification, and pure heave. The first two components refer to temperature and salinity changes that occur without a change in density; because the equation of state for seawater is a nonlinear function of temperature, salinity, and pressure, there are several combinations of temperature and salinity that yield the same density. These changes in temperature and salinity are now commonly referred to as water property changes, or *spice*. Pure heave is defined as the vertical displacement of isopycnals with no changes in temperature and salinity characteristics.

Several studies have used this heave/spice decomposition to distinguish changes in the ocean. *Bindoff*

and McDougall (1994) included a study in the Tasman Sea at 43°S, which found that seasonal variability was mostly owing to heave, whereas multidecadal changes were explained by spice. Global ocean data has shown multidecadal warming at shallow depths (0-700 m) as well as the warming and volume expansion of subtropical mode waters. This layer expansion produced a large, warming-associated heave signal, especially in the Southern Hemisphere, along with an enhanced spice contribution to warming in the Southern Ocean (*Häkkinen et al.*, 2016).

McDougall and McIntosh (2001) created a variation of this methodology to quantify heave due to mesoscale eddy activity in models, incorporating heave and ocean velocity. A later study used this technique to study eddies in the global Argo dataset, and showed enhanced heave due to eddy activity near the Antarctic Circumpolar Current and strong western boundary currents such as the Gulf Stream (*Katsumata*, 2016).

This method of decomposing ocean variability into heave and spice has been useful for describing ocean variability in several studies, but it has some concerning drawbacks. Firstly, the distinction between heave and spice is unclear because it is possible for pure heave to induce spice changes. An isopycnal can heave for two reasons: due to the movement of a water mass, or due to a change in the properties of the water mass. Because potential density depends on temperature, salinity, and pressure, the vertical movement of water can lead to changes in temperature and salinity, especially in the presence of strong temperature and salinity gradients. Thus separating heave and spice in this way can lead to mischaracterization of heave and spice.

Secondly, this method measures heave in terms of potential density, which can mask temperature and salinity variability. Small changes in temperature and salinity may not be detectable after converting to potential density, but these small variations can be important indicators of both vertical and lateral motion in the water column. It would therefore be advantageous to instead measure heave based on independent temperature and salinity measurements, so that vital information will not be excluded.

It is also important to note that this decomposition into heave and spice does not represent a distinction between natural and climatic variability. Although *Bindoff and McDougall* (1994) found that spice in the Tasman Sea played a larger role in density variability than heave on multidecadal timescales and hypothesized that these spice changes were related to climatic changes, the association between spice and long-term climatic

changes is not the case everywhere. Other studies have found considerable short-term oscillations in spice, meaning heave or spice is not inherently associated with either natural or climatic variability (*Bryden et al.*, 2003). There is nothing inherent about heave or spice that is tied to climatic or natural variability. Spatial-temporal analyses of the movement of water masses and changes in water mass properties is required to distinguish natural versus climatic influences on the ocean.

1.4.2 Isotherm Heave

Purkey and Johnson (2013) used a variation of the *Bindoff and McDougall* (1994) heave and spice decomposition by focusing on potential temperature rather than density, i.e. measuring isotherm heave instead of isopycnal heave. They used this approach for a study on Antarctic Bottom Water, because small salinity changes led to much larger error in heave calculations in the deep Southern Ocean.

The isotherm heave methodology may be an improvement upon *Bindoff and McDougall* (1994) in that it uses independent temperature and salinity measurements, rather than conflating the two in potential density. However, it is limiting in that it expresses all the water property changes (spice) in terms of salinity, and all the heave is attributed to temperature changes (*Purkey and Johnson*, 2013). It is unlikely that spice or heave is influenced solely by temperature or salinity, and isolating each term can exclude potentially useful information about temperature and salinity changes. Though this approach was useful for handling salinity noise in the highly unstratified Southern Ocean, it is probably not generalizable for use in the global ocean, which varies greatly in stratification.

1.4.3 Accounting for the Lateral Movement of Isopycnals

Durack and Wijffels (2010) critiqued the methodology of *Bindoff and McDougall* (1994) because it did not account for the lateral movement of isopycnal surfaces. Measuring heave in just the vertical dimension does not capture the movement of isopycnal surfaces, which are really in three dimensions. *Durack and Wijffels* (2010) amended this by computing the time-averaged location of isopycnals in three dimensions and measuring deviations from their average location. This separated heave into vertical and lateral components, along with spice. They found significant poleward lateral migration of isopycnals (50-100km) associated with long-term warming, and showed that changes in isopycnals on this scale can have a large influence on ocean

circulation (*Durack and Wijffels*, 2010).

This methodology is noteworthy because it improves on the methodology of *Bindoff and McDougall* (1994) by treating isopycnal heave as a three-dimensional phenomenon. We only address vertical heave in our work, but measuring heave in three dimensions would be a clear next step.

1.4.4 Excluding Heave by Using T-S Space

To avoid the influence of heave and focus only on water property changes, *McDonagh et al.* (2005) quantified temperature and salinity changes along isopycnals by computing a least-squares distance between chronological temperature-salinity curves. This technique attempts to study spice without the influence of heave, but as noted earlier regarding the heave/spice decomposition in *Bindoff and McDougall* (1994), heave and spice are not completely independent processes. This approach also likely does not completely remove the heave signal from the spice signal, and is worth noting because it is commonly used in oceanographic studies.

1.5 A Novel Approach

We provide an alternative approach for quantifying isopycnal heave while improving upon previous methods. Our methodology uses both isohalines and isotherms (surfaces of constant salinity or temperature), thereby using more information than potential density alone. We also prioritize the applicability of our technique across the global ocean, to measure heave in various types of stratification and ocean profiles. Our approach uses a novel application of dynamic warping to measure heave accurately, even with noisy data in regions with low stratification where small changes in temperature and salinity may be interpreted as large vertical heave.

Our work also studies the ability of the Argo array to quantify heave in the global ocean. We do this by comparing Argo data, which is sporadically sampled spatially and temporally, to regularly-sampled station datasets in the Pacific and Atlantic oceans that reach down to the ocean floor. Comparing the heave estimates from the float data and the station data help us determine whether the Argo data can sufficiently measure the heave processes occurring in a particular region. Looking at the variability of heave with depth can also show how the lower range of the Argo data may be indicative of heave in the deeper ocean, beyond the depth

of Argo's sampling range.

The structure of this thesis is as follows. Chapter 2 compares the conventional method for measuring heave (as described in *Bindoff and McDougall* (1994)) to the novel methods we developed. Chapter 3 applies these heave estimation methods to station data near Hawaii and Bermuda to characterize the vertical and temporal structure of heave through the entire water column. Chapter 4 shows correspondence between heave estimates from the stations and nearby Argo data, demonstrating the potential to use Argo data to characterize heave throughout the world oceans. Chapter 5 discusses the application of our novel heave estimation method to the Argo data in the North Pacific Ocean, including the influence of various natural and climatic ocean processes on heave and an ocean heat uptake calculation. Chapter 6 summarizes main takeaways from our work and proposes future directions of study.

Chapter 2

Measuring Heave

In this study, we explore alternative ways to measure heave because the conventional use of potential density can mask much of the variability present in independent temperature and salinity measurements. Here we describe our implementation of the conventional heave-spice decomposition methodology and our novel techniques for quantifying heave.

The convention in the literature is to define downward movement of isopycnals as positive heave, because it is associated with a positive temperature change; however, we choose to instead define upward movement as positive heave.

2.1 Methods

2.1.1 Conventional Potential Density Method

The conventional method for measuring heave, as described by *Bindoff and McDougall* (1994), measures the change in pressure along isopycnal surfaces over time. Since pressure is analogous to depth, we interpret heave in depth units (meters) rather than pressure units (dbar) and convert pressure to depth for our calculations.

We implement this method by converting potential temperature and salinity profiles to potential density profiles with a reference pressure of 2000 dbar (σ_2), and measuring the depth offset between the profiles (Fig. 2.1). This requires interpolating the sample potential density profile onto the reference (time-averaged) potential density profile, then calculating the depth difference between the profiles. We interpret this depth difference as heave. Notice how in low stratification, small changes in density can make a large difference in heave (Fig. 2.1).

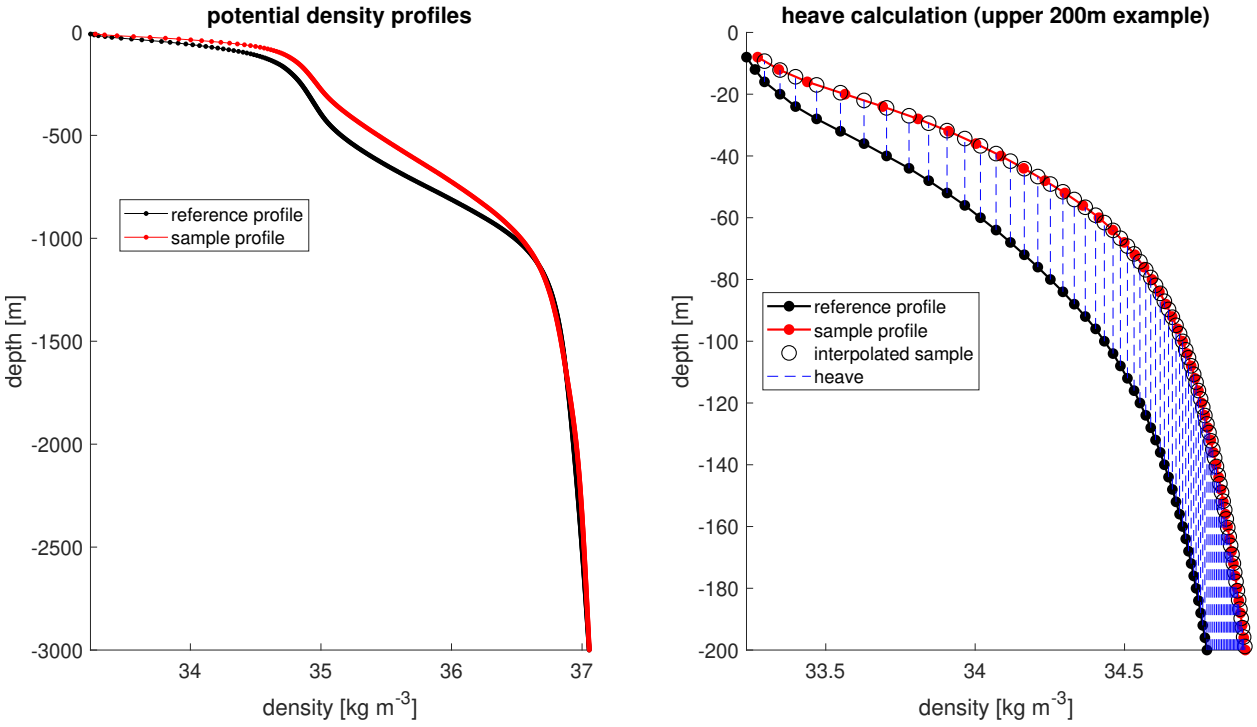

Figure 2.1: Conventional method for estimating heave, using potential density. Left: Example potential density profiles derived from the Bermuda Atlantic Time Series. Heave is calculated from the sample profile (red) relative to the reference profile (black). Right: Heave (blue dotted lines) is the depth offset between the sample and reference profile.

We also calculate spice in a similar way to the heave calculation. We interpolate the sample temperature and salinity onto the mean potential density profile, then measure the temperature and salinity change at each density point.

2.1.2 Dynamic Depth Warping

Our novel method for measuring heave uses a linear programming technique called dynamic warping. Dynamic warping is a way of comparing two sequences of linear data that are similar in shape, by identifying their similar structures and stretching and squeezing the data to achieve an optimal alignment. This warping technique is most often used with timeseries data (Dynamic Time Warping), to minimize unwanted speed or temporal offsets as a way of standardizing signals such that their characteristics can be more easily compared

(*Berndt and Clifford*, 1994). A common application of Dynamic Time Warping is speech recognition; the warping algorithm can compensate for varying speeds of speech to recognize structures that represent certain words.

Dynamic warping also calculates the offsets that are needed to align the signals at every point in the data. Though most applications of Dynamic Time Warping are not interested in these offsets, they are useful in our application of dynamic warping to vertical ocean profiles. Instead of measuring temporal offsets at every time-step in two timeseries, we quantify depth offsets (heave) at every depth of interest in two ocean profiles. We call our application of dynamic warping to ocean profiles Dynamic Depth Warping (DDW), because the warping occurs in the depth dimension. This approach is useful because we want to quantify offsets between ocean profiles purely in the depth dimension, not the changes in the shapes of the profiles due to temperature or salinity changes (i.e. water mass changes).

DDW accepts two inputs, a sample profile and a reference profile. The reference profile is generally a time-averaged profile in the region of interest so we can track heave anomalies over time by calculating heave between many samples and the reference profile. DDW first computes the distance between every data point in both profiles, forming a distance matrix (Fig. 2.2). DDW then finds the unique path of lowest cumulative distance through the distance matrix, known as the *warping path*. The warping path describes the nonlinear adjustments required to align the profiles in the depth dimension; converting the warping path to depth coordinates yields the depth offsets (heave) between the profiles in meters through the entire water column. DDW also has an option to include a penalty term that prevents the warping path from straying too far from the 1-to-1 line. We find that including a small penalty term in the warping process is useful for handling noisy ocean data.

By using DDW to compare each profile to a time-averaged mean profile, we can calculate heave through the entire depth of the water column over time (Fig. 2.3). We set the surface as a closed boundary assumed to have no heave, and left an open boundary at depth, because the profiles we use in practice are cut off several hundred meters above the ocean floor. This means the net heave calculated for each profile may be nonzero. We apply DDW to temperature and salinity profiles independently to measure heave before incorporating the two with a more advanced version of this technique.

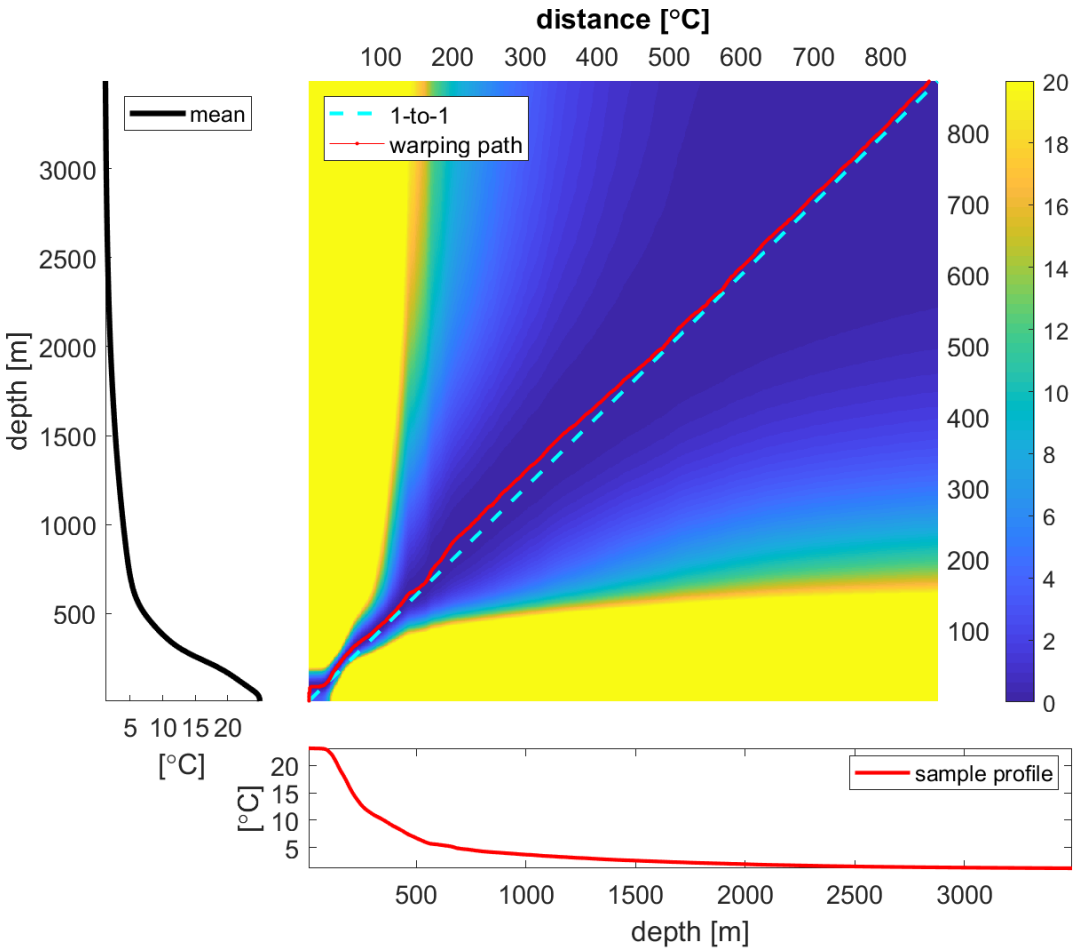

Figure 2.2: Distance matrix and warping path generated by Dynamic Depth Warping for two temperature profiles. DDW calculates the distance (color) between every point in the reference, or mean profile (left, black) and the sample profile (bottom, red). The path of least cumulative distance through the distance matrix (red) is the *warping path*. When the warping path deviates from the 1-to-1 line (cyan dashed), warping was required to align the profiles.

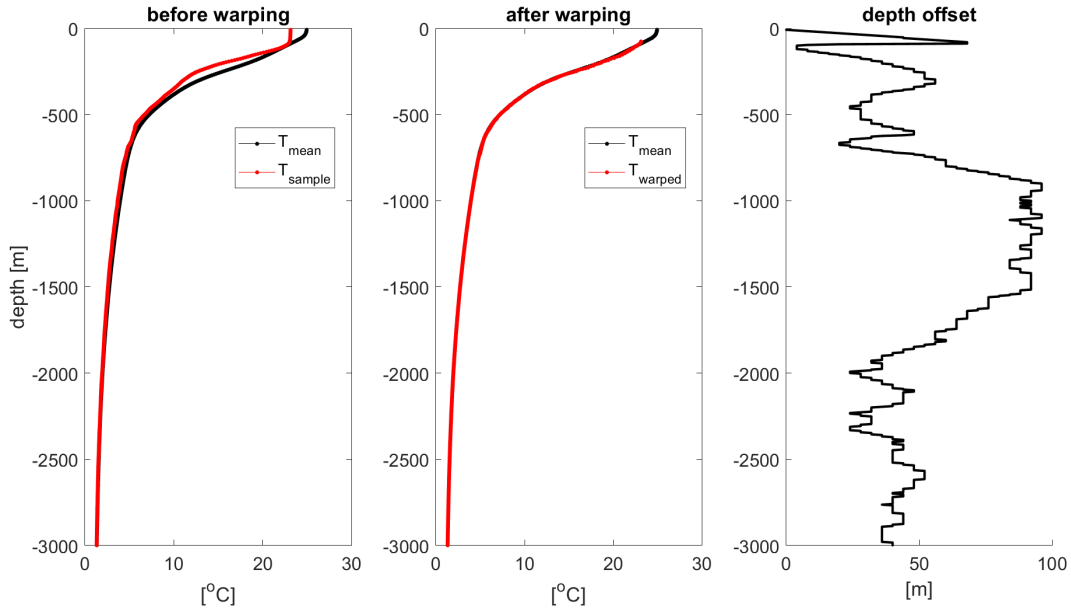

Figure 2.3: Dynamic Depth Warping. [Left] Mean temperature profile and a sample temperature profile from one time interval in the Hawaii Ocean Timeseries data, [Center] the aligned profiles generated by dynamic warping, [Right] the vertical offset (heave) between the two profiles as a function of depth.

2.1.3 Dual-Dynamic Depth Warping

We further develop this novel method for estimating heave by incorporating independent temperature and salinity measurements into a simultaneous warping algorithm, and call this method Dual-Dynamic Depth Warping (Dual-DDW). Dual-DDW generates the distance matrices for temperature and salinity independently, combines the distance matrices with a weighting to account for the difference in units between temperature and salinity, then calculates the warping path through the combined distance matrix. This allows the heave estimate to be influenced by both temperature and salinity without one overpowering the other.

The weighting between the temperature and salinity matrices is determined by comparing the change in potential density due to a one-unit change in temperature versus a one-unit change in salinity. The weighting increases the influence of salinity because salinity changes in the ocean are very small compared to changes in temperature, but the salinity distance matrix is not weighted so much that small salinity changes overpower

the warping. This weighting is adjustable, but since we mostly apply this method to the deep ocean where temperature and salinity changes are small, we keep this weighting consistent for all depths.

Dual-DDW can also detect variations in temperature and salinity that cannot be explained by vertical heave, but rather indicate horizontal advection. This occurs when a water column is laterally intruded by a water mass with different temperature and salinity characteristics from the local waters. Figure 2.4 shows an example of this around 200-400m depth, and the intruding water mass is especially evident in the salinity profile. When this happens, there is a large jump in the heave estimate in only a few meters depth, which is nonphysical. This indicates that something other than vertical changes is affecting these profiles. In this example, Dual-DDW does not quite pick up on the large jump in salinity, but this may be due to the weighting being calibrated for the deeper ocean where temperature and salinity gradients are smaller.

This technique is useful because it uses information from both temperature and salinity, which allow for better detection of vertical changes than a solely density-based technique. The presence of a foreign water mass is typically clear in temperature and salinity profiles, but the density profile may show barely any change because the water mass will intrude along an isopycnal with density characteristics similar to its own. Using independent temperature and salinity data rather than only density data is therefore very useful for distinguishing between vertical heave and horizontal advection. This Dual-DDW approach can potentially provide more accurate heave estimates and additional insight into the physical mechanisms influencing ocean measurements.

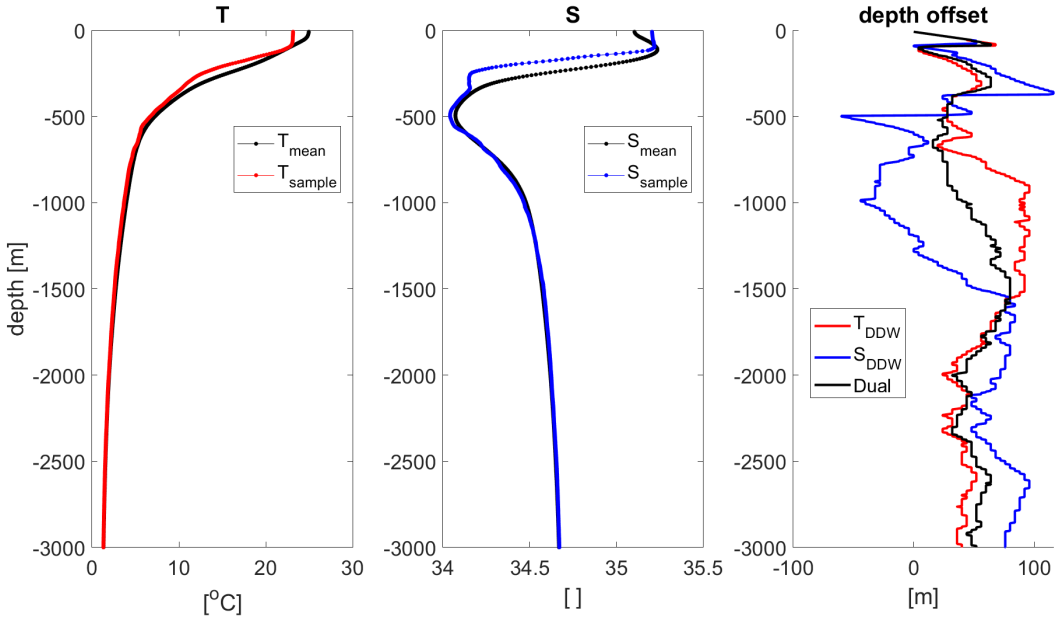

Figure 2.4: A comparison of warping methods to calculate heave for one vertical profile. [Left] Mean temperature profile and a sample temperature profile from the Hawaii Ocean Timeseries, [Center] as left but for salinity, [Right] vertical offset (heave) between the sample and mean profiles as a function of depth, calculated by warping temperature, salinity, and temperature and salinity simultaneously with Dual-Dynamic Depth Warping.

2.1.4 Potential-Density Warping

The final method we use to calculate heave is warping the potential density profiles. The methodology is the same as temperature warping or salinity warping, only applied to potential density. We include this technique to make a more direct comparison between our temperature and salinity-based heave calculations and the potential density-based heave calculations.

2.2 Results

To evaluate the performance of these methods for estimating heave, we heave temperature and salinity profiles synthetically, use each method to estimate the heave between the synthetically-heaved profiles, and compare the estimates to the actual synthetic heave that we prescribed. The temperature and salinity profiles

we use for these synthetic tests are the time-averaged profiles from the Hawaii Ocean Timeseries (HOT) and the Bermuda Atlantic Time-series Study (BATS), two stations in the north Pacific and Atlantic oceans that have been collecting monthly CTD profiles down to the ocean floor since the late 1980s. These datasets are described and analyzed in further detail in Chapter 3, but here we simply use the mean profiles from each station to test our heave estimation methods with multiple types of ocean profiles.

The mean profiles from these datasets are considered the "reference profiles." We then add depth offsets (heave) to these temperature and salinity profiles, ensuring that the heave at the surface is equal to zero. The heaved profile, which we call the "sample," is then reinterpolated back onto the original depth space. We then use each heave method to calculate the heave between the reference and the sample (heaved) profile. For the conventional potential-density method from *Bindoff and McDougall* (1994), we calculate both heave and spice. Sections 2.2.1 and 2.2.2 show the results of these tests for Dual-Dynamic Depth Warping (Dual-DDW), potential density warping, and the conventional potential density method.

2.2.1 Synthetic Heave Test: Heave and Spice

In our first synthetic tests, we want to (1) measure the accuracy of each heave estimation method, and (2) determine whether pure heave can cause spice changes. We do this by synthetically creating a smooth heave profile with depth, by adding together several sine waves and ranging the amplitude between 0-200m, which is the typical magnitude of heave in the ocean. We then apply this heave to the mean profiles from HOT (Fig. 2.5) and BATS (Fig. 2.6). Because we know exactly what heave was applied to these profiles, we can compare the output of each heave estimation method to the actual heave and determine an error. We also use the conventional method from *Bindoff and McDougall* (1994) to calculate spiciness; if heave and spice were truly distinct, the spice in this synthetic test would be zero because we only heaved the profiles.

The first important result from this test is that the pure heave we apply to the HOT and BATS profiles produces nonzero spice. This provides further evidence that heave and spice as defined in *Bindoff and McDougall* (1994) are not completely distinct. As expected, heave causes the most spice at depths with large salinity and temperature gradients, such as above 500m in the HOT profiles (Fig. 2.5e) and in the upper 100m and mid-depths between 500-1000m in the BATS profiles (Fig. 2.6e). The heave-induced spice is also very large, with a nearly 6°C cooling and 1 salinity unit of freshening for the HOT profiles. The spice

changes are substantial but smaller in the test with the BATS profiles, with just over 2°C of cooling and 0.5 salinity units of freshening. However, the spice would likely be larger in the BATS test if the depths with large synthetic heave matched the depths with strong temperature and salinity gradients, as is the case in the test using the HOT profiles.

The second result from this test is that the error between the synthetic heave and the heave estimates for all three methods is very small. The error for the conventional density method is nearly zero, while the error for the warping methods oscilllates between ±2m. Heave in the ocean is usually on the order of tens to hundreds of meters, so in that context this small difference in error is negligible. Additionally, the error for the warping methods is dictated by the depth resolution of the data, and the error can therefore be adjusted with depth interpolation. Warping occurs when there is a detectable depth offset between the profiles, but the warping occurs at the same resolution as the depth resolution (in this case, 4m increments). Profiles can therefore be offset by up to 2m without being detected by the warping method as needing to be warped, hence the error associated with our warping methods will be half of the depth resolution. To make a fair comparison between our warping methods and the conventional potential-density method for estimating heave, we use a depth resolution of 4m to produce an expected error of ±2m for all the synthetic tests and data analysis in this study.

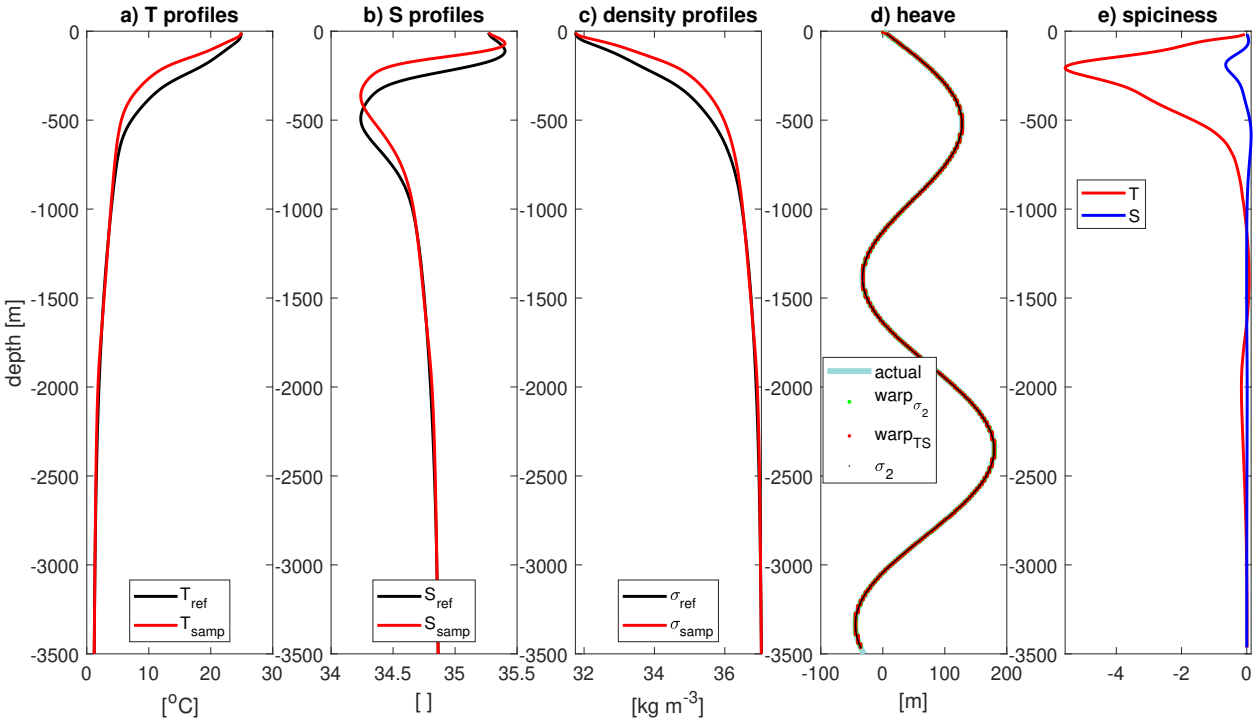

Figure 2.5: a) Mean temperature profile (black) from the Hawaii Ocean Time-Series and synthetically heaved profile (red). b) As a) for salinity. c) As a) for potential density (σ_2). d) Synthetic heave applied to the profiles (blue line) and heave estimated using density warping (green), Dual-DDW (red), and the conventional potential density method (black). Blue line is thick for visibility, but represents a single heave value at each depth. e) Spiciness change in temperature (red) and salinity (blue), with °C and salinity units on the same axis.

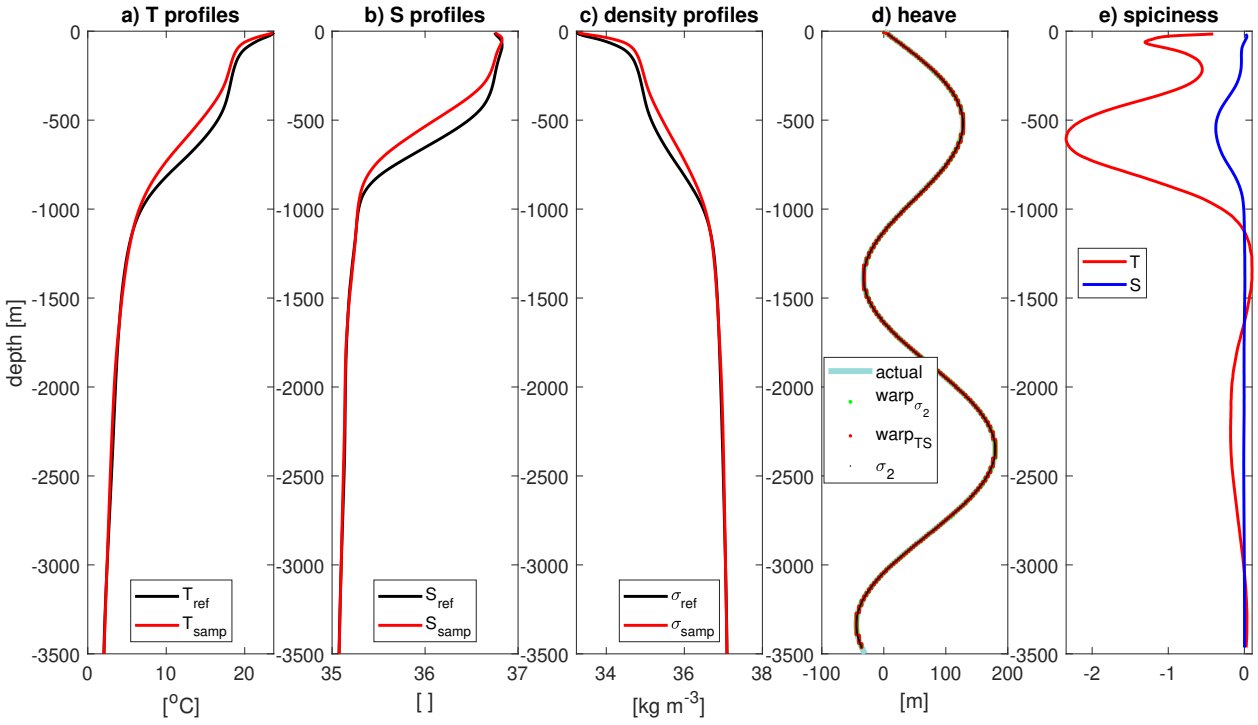

Figure 2.6: As Fig. 2.5, using the Bermuda Atlantic Time-series Study (BATS) mean profiles.

2.2.2 Synthetic Heave Test: Adding Noise

Our next synthetic test aims to determine how well the heave estimation methods perform in the presence of noise. When we apply these methods to real data, the profiles will not be smooth as they were in the previous synthetic test. Though the real data could have noise or jumps for a variety of reasons, here we only introduce a small amount of noise in accordance with the accuracy of the CTD sensors used in the stations and Argo. Various dynamic errors can cause salinity errors ranging from 0.005-0.02 salinity units, and friction with water flowing through the sensor at a speed of 1 m/sec can cause a slight heating of 0.001-0.002°C (noa, 2016). We choose to use the low end of this error for salinity and the high end for temperature in attempt to balance out the errors between temperature and salinity, but ultimately the larger errors from salinity have a disproportionate effect on the profiles. We add a uniform distribution of salinity error between ± 0.005 units to the salinity profiles, and up to 0.002°C of heating to each point in the temperature profiles.

There are also differences in error between the three heave estimation methods (Fig. 2.9). When we

conduct many iterations of this synthetic test with noise, the conventional potential density method has a much wider distribution of error than the density and Dual dynamic warping methods. The error from the conventional method ranges from ±30m in intermediate/deep depths to ±100m below 3000m. These are very dramatic errors in the context of heave in the real ocean, which we expect to be on the order of 50-200m.

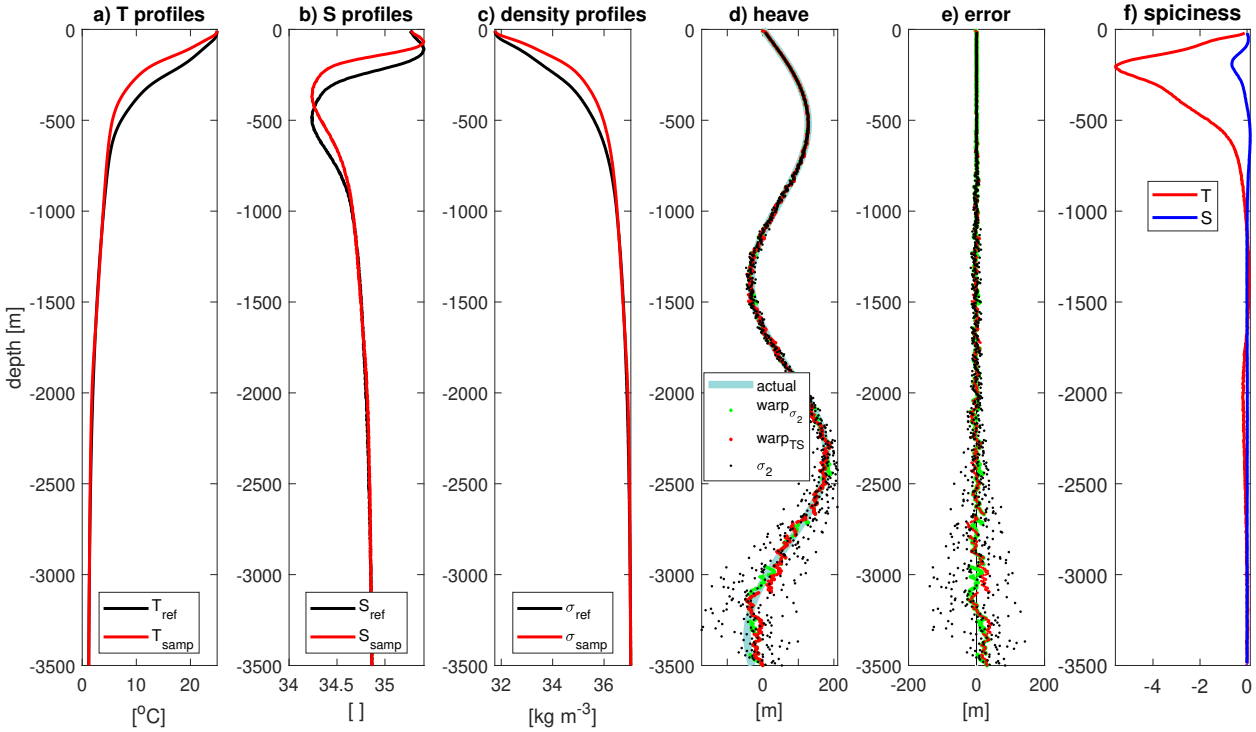

Figure 2.7: Synthetic heave test with noise introduced into the temperature and salinity profiles. a) Mean temperature profile (black) from the Hawaii Ocean Timeseries (HOT) and synthetically heaved profile (red). b) As a) for salinity. c) As a) for potential density (σ_2). d) Synthetic heave applied to the profiles (blue line) and heave estimated using density warping (green), Dual-DDW (red), and the conventional potential density method (black). e) The error between the synthetic heave and the heave estimated by each method. f) Spiciness change in temperature (red) and salinity (blue), with °C and salinity units on the same axis.

The density warping method and the Dual-DDW method yield similar error on average with depth, but there are some subtle differences between the Hawaii and Bermuda tests. In the case of the synthetic test using the HOT mean profiles, the density warping error distribution is slightly narrower than that of Dual-DDW (Fig. 2.9a). Conversely for the synthetic test using the BATS profiles, the Dual-DDW error

distribution is narrower than that of the density warping method (Fig. 2.9b). This may indicate that there is variation in the warping methods' performance for differently-shaped profiles; perhaps there is a relationship between error distribution and profile stratification. This is an important direction for future study.

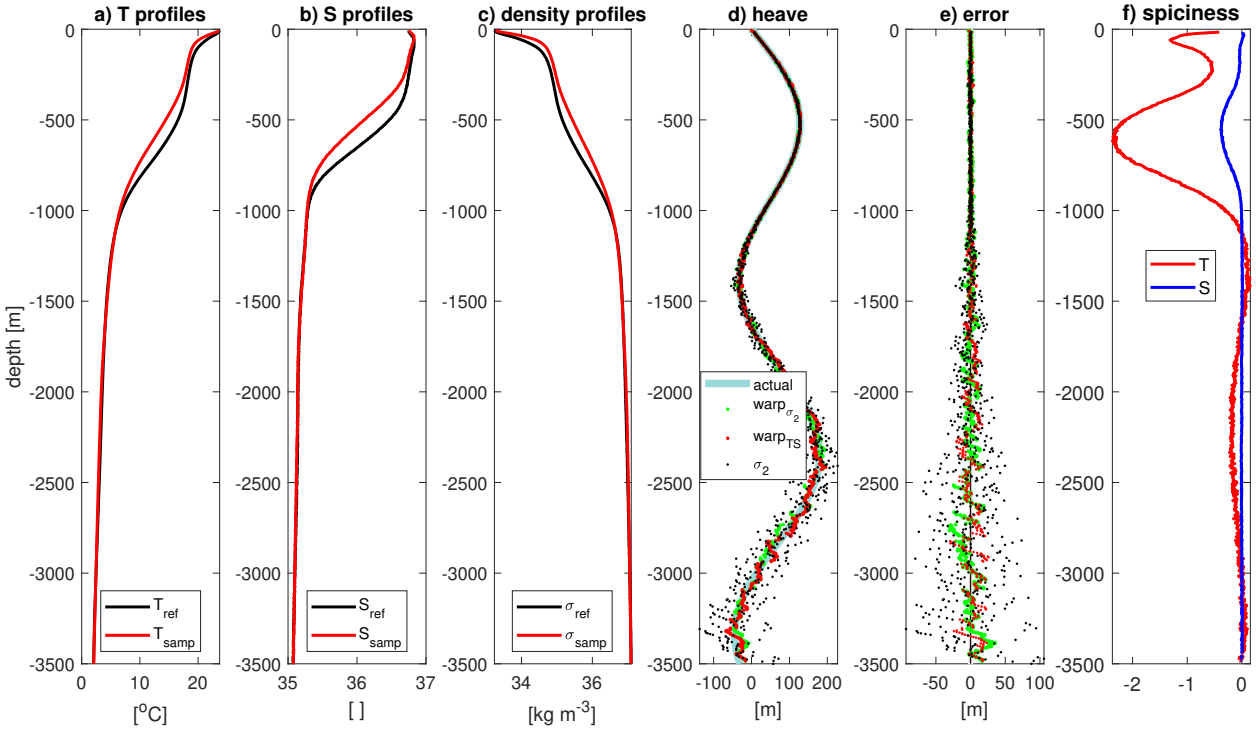

Figure 2.8: As Fig. 2.7, using the Bermuda Atlantic Time-series Study (BATS) mean profiles.

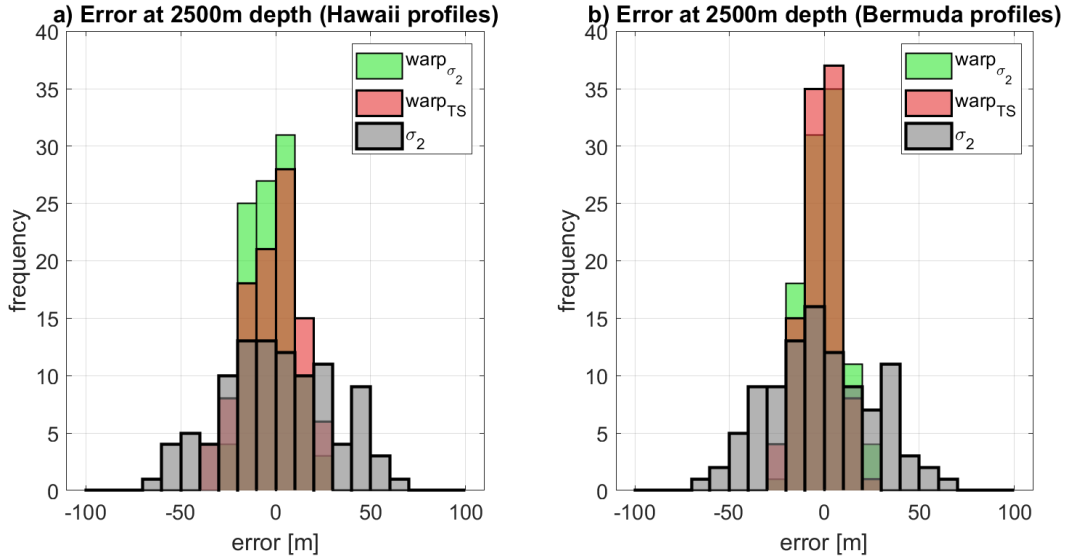

Figure 2.9: Distribution of error from the synthetic test with noise at 2500m depth for 100 iterations of the test. Distributions for each heave estimation method are shown: density warping (green), Dual-DDW (red), and the conventional potential density method (black). a) For the synthetic noise test using the Hawaii Ocean Timeseries (HOT) mean profiles. b) For the synthetic noise test using the Bermuda Atlantic Time-series Study (BATS) mean profiles.

2.3 Discussion

The mean profiles from HOT and BATS are only two types of ocean stratification and do not represent the entire ocean. However, they help us understand how our heave estimation methods work. Our tests without noise showed that pure heave could induce spice changes, and therefore the conventional decomposition of heave and spice is misguided. In the test where we added noise in the temperature and salinity profiles, the error for all three methods increased, but especially that of the conventional potential density method. More could be done to quantify these methods' sensitivity to stratification, but in general the error for each method increases as stratification decreases. The density warping method and the Dual-DDW method tend to have similar magnitudes of error for the locations we tested, though this might be different for differently-shaped profiles in other locations and requires further investigation. Overall, these results show that both of the warping methods are likely accurate ways of estimating heave, and will probably be much more accurate

than the conventional method when we apply them to real data.

Chapter 3

Vertical Structure of Heave in Station Data

Having demonstrated that our methods for calculating heave are reliable with synthetic data, we can now apply our methods to real data and characterize heave throughout the water column. A good starting point is to use data collected from stations, because station observations can track changes in the ocean at the same location over time. There are two stations in the North Pacific and Atlantic oceans that have been collecting full-depth CTD (Conductivity, Temperature, Depth) profiles at monthly resolution for over three decades. Calculating heave at these stations from the surface to the deep ocean would be an appropriate starting point for our data analysis. Characterizing heave in these basins will also be useful information when we want to expand our analysis to the Argo dataset.

3.1 Data

3.1.1 Hawaii Ocean Timeseries

The Hawaii Ocean Time Series (HOT) is a multi-decadal dataset consisting of monthly physical, chemical and biological ocean measurements. The program was created in 1988 to provide long-term comprehensive data records for studying water masses, climatic variability, carbon and potential human impacts on the ocean. The data was collected at Station ALOHA, which is located at (22°45'N, 158°W), about 100 km North of O'ahu and 50 km away from the bathymetry of the Hawaiian Ridge that would influence nearby observations (Fig. 3.1). Station ALOHA is located in deep water (4800 m), allowing data to be collected in large vertical profiles. For this study, we used the temperature and salinity profiles from HOT collected from 1988-2016.

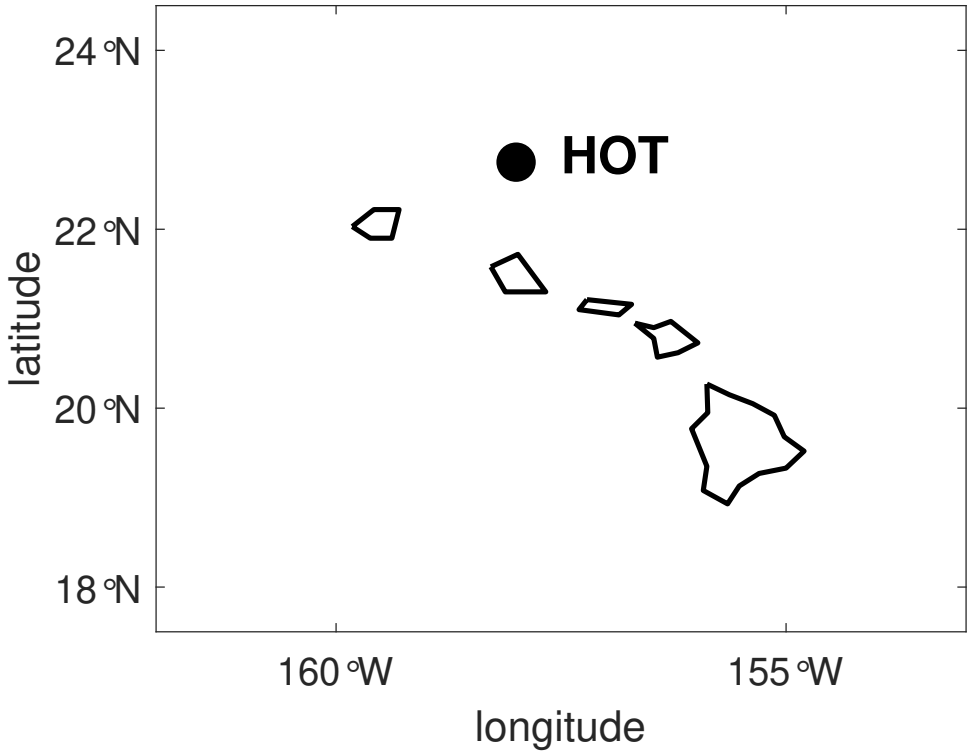

Figure 3.1: Location of the Hawaii Ocean Timeseries (HOT) station near the Hawaiian islands.

There are several things we might expect to find when we calculate heave in the HOT data. The seasonal subduction of warm surface waters has been found to be a very small signal in this region, so the heave associated with this process should be restricted to the upper 10-120m of the ocean (*Karl and Lukas*, 1996). Recurring Rossby waves with a period of 100-130 days have been found north of the HOT station with satellite altimetry data (*Mitchum*, 1996). The HOT data has also shown interannual changes in the temperature of deep and abyssal water masses, with variation on 2 and 3-year timescales respectively (*Lukas and Santiago-Mandujano*, 1996). These temperature changes were attributed to Rossby waves associated with the El Niño-Southern Oscillation (ENSO), an irregular oceanic and atmospheric change that occurs every few years in the Pacific Ocean, as well as interannual wind changes in the regions where these deep water masses form. These temperature changes were estimated to have been associated with isotherm heave on the order of 150m in the deep ocean (∼3500m depth) and 300m in the abyssal ocean (∼4500m depth). The high heave in the abyssal ocean, along with the fact that the HOT station is surrounded by shallower

waters, indicated that perhaps horizontal advection also played an important role in abyssal water mass variability (*Lukas and Santiago-Mandujano*, 1996).

In examining the temporal variability of heave in the HOT data, we choose to examine the upper 3000m to avoid the aforementioned effects of horizontal advection. We should expect to find annual variability above 120m depth, higher-frequency variability with a period of 100-130 days, and low-frequency variability with 2-3 year periods at depth.

3.1.2 Bermuda Atlantic Time-series Study

The Bermuda Atlantic Time-series Study (BATS) began in 1988 with the intent to study biogeochemical changes in the ocean on seasonal, interannual, and decadal timescales (*Michaels and Knap*, 1996). The ocean's role in the global carbon cycle and heat uptake were two primary motivators for establishing BATS. The BATS station is located at (31°40'N, 64°10'W), 85 km southeast of Bermuda in the Sargasso Sea above relatively flat topography. The BATS station measurements can reach down to 4200m depth.

The region where BATS is located is characterized by more complex ocean variability than the region where HOT is located. The Sargasso Sea often experiences local fluctuations on the scale of days to weeks, as well as the common presence of eddies and the lateral advection of water (*Michaels and Knap*, 1996). This high-frequency variability and horizontal advection may prove challenging and even problematic for our vertical heave analysis; short-lived fluctuations in heave can make it more difficult to examine heave trends, and horizontal advection could be misinterpreted as vertical heave. In our analysis, however, we address these concerns carefully.

Seasonal variability associated with the subduction of warm surface waters is expected in the upper few hundred meters of the BATS data, because the mixed layer is deeper here than near Hawaii and the HOT station (*Michaels and Knap*, 1996). Due to seasonal changes in winds in the North Atlantic that influence the formation of North Atlantic Deep Water, seasonal variability is also expected in the deep ocean in the BATS region. This water mass subducts into the deep Atlantic near Greenland and travels towards the Equator, carrying seasonal variability along with it (*Johnson and Marshall*, 2002). We thus expect to see seasonal heave in areas containing North Atlantic Deep Water, including the Sargasso Sea (*Nieves and Spall*, 2018). Additionally, upper ocean mixing in the BATS data has been shown to correspond with ENSO (*Michaels*

and Knap, 1996).

We expect to observe heave on seasonal scales in the surface and deep ocean, ENSO (interannual) variability in the upper ocean, and high-frequency variability at many depths in the BATS data.

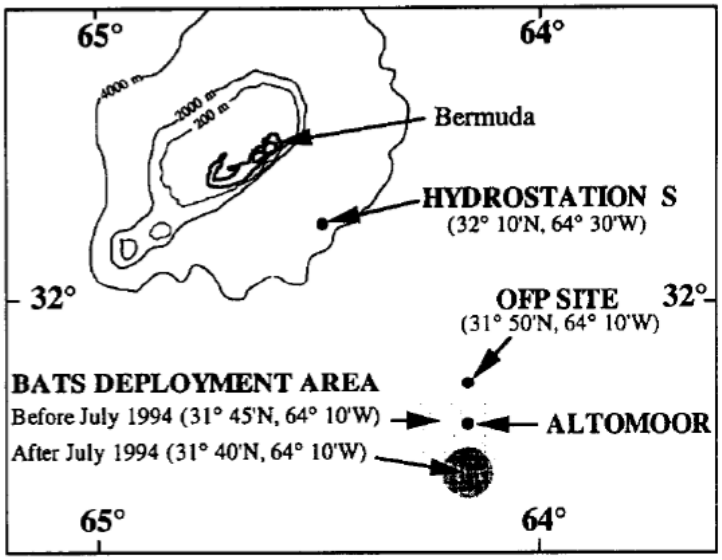

Figure 3.2: Location of the Bermuda Atlantic Time-series Study (BATS) station in the Sargasso Sea near Bermuda. Various other observing sites are also shown. From *Michaels and Knap* (1996).

3.2 Methods

3.2.1 Depth Interpolation

The original form of the HOT and BATS data had approximately 10m depth resolution. In line with our synthetic tests from Chapter 2.2.1, we linearly interpolate the HOT and BATS data to 4m depth resolution. This makes the error in the warping methods small enough to ensure a fair comparison with the conventional potential density method.

3.2.2 Singular Value Decomposition

Singular Value Decomposition (SVD) allows us to characterize heave patterns in the HOT and BATS data. Each heave estimation method applied to many samples over time outputs a heave matrix H, with rows representing depth levels and columns representing samples (time).

H can be rewritten as the product of three matrices:

$$H = U\Sigma V^T$$

where the columns of U describe the vertical structure of heave and the columns of V describe the temporal structure of heave. The columns of U and V are orthonormal and describe independent patterns of variability in the data. Σ is a diagonal matrix containing the squared eigenvalues of H, and explains how much each column of U and V contributes to the variability of the data.

To distinguish the vertical and temporal variability of heave as described by U and V, we tend to refer to the columns of U as "vertical modes" or "principal components" of heave, whereas we refer to the columns of V as EOFs (Empirical Orthogonal Functions). Since the first few columns of U and V represent most of the variability of the heave in HOT and BATS, we focus on these elements for our analysis.

3.2.3 Multi-Taper Spectral Analysis

Spectral analysis describes how strongly different periods of variation are expressed in a signal. It is often used to understand the periodic processes that influence a system. A spectral peak at a particular frequency indicates that the data vary at that frequency. Analyzing the heave in HOT and BATS using spectral analysis helps us identify the periodicity of the heave at different frequencies. Knowing the dominant frequencies of heave helps us identify which oceanic or atmospheric processes are influencing the data.

We first apply spectral analysis to the first EOF (first column of V) from the SVD output. The first column of U and V explain the most variance of the dataset, so conducting spectral analysis on the first EOF helps to isolate the main heave pattern in the station data and understand its temporal structure. We then apply spectral analysis to the raw output from Dual-DDW and density warping for a variety of depth

ranges, to determine how the temporal variability of heave changes with depth.

3.3 Results

3.3.1 Hawaii Ocean Timeseries

In the case of the Hawaii Ocean Timeseries (HOT) station, the main pattern of heave is increasing magnitude with depth, as shown by the first principal component of vertical heave variability from SVD (Fig. 3.3c). This pattern explains approximately 73% of the heave variability in the HOT data. Heave in the upper 500m of the HOT data tends to be less than 50m in amplitude, but heave near 2000m can reach 100m in magnitude, and in the deep ocean near 3700m depth, heave regularly exceeds 100-150m. This magnitude of heave aligns with previous estimates of isotherm heave required to explain the temperature variability at these depths (*Lukas and Santiago-Mandujano*, 1996). The large heave at depth is likely due to the decrease in stratification with depth in this region (Fig. 3.3a & b). Low stratification allows internal waves and other disturbances to have a larger vertical influence, because it is easier to heave water vertically when it is not restricted by a density gradient.

All three heave estimation methods (Dual-DDW, density warping, conventional method) yield nearly identical heave estimates for the HOT data (Fig. 3.3). Keeping this similarity in mind, all of the temporal analysis will be conducted using the heave calculated by our novel method, Dual-DDW.

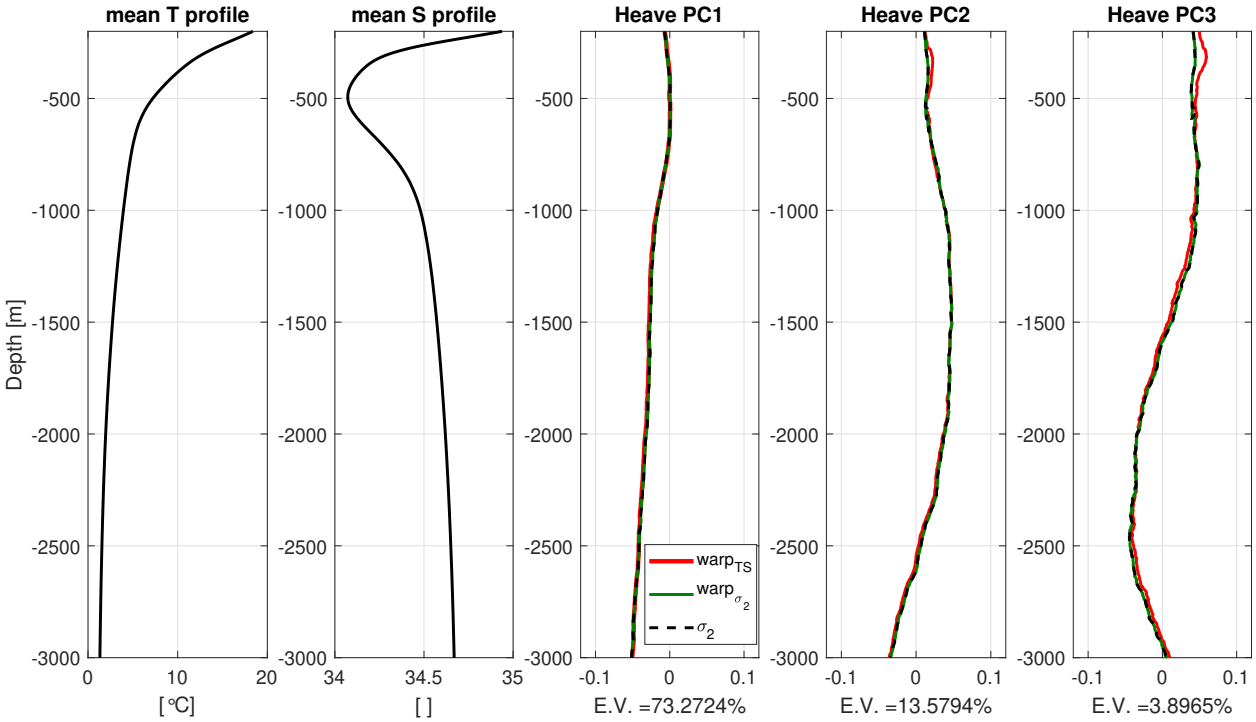

Figure 3.3: For the heave calculations in the Hawaii Ocean Timeseries: Mean temperature and salinity profile averaged over 1988-2016, and the three most dominant principal components of heave as generated by singular value decomposition. E.V. refers to the explained variance of each principal component, as calculated by Dual-Dynamic Depth Warping. Colors refer to the different methods for estimating heave, Dual-DDW (red), potential density warping (green), and the conventional potential density method (black dashed).

When we examine heave at many depth levels, we find that different frequencies dominate the power spectra at different depths (Fig. 3.4). The seasonal cycle has a very distinct peak at 100m depth, and this peak disappears below the surface ocean. This is surface restriction expected because the layer in the surface ocean with low stratification which experiences large seasonal variability (also known as the mixed layer) is shallow in this region. There is a broad peak around 1 cycle/3 yr frequency that appears around 2000m depth and continues to be present through 3500m depth. This looks more like a continuum of variability rather than a peak, indicating there may be multiple processes influencing heave at these depths, or a process that occurs with inconsistent frequency, such as ENSO. This broad peak at depth could also be related to wind changes that affect deep waters near Hawaii, as noted in *Lukas and Santiago-Mandujano* (1996).

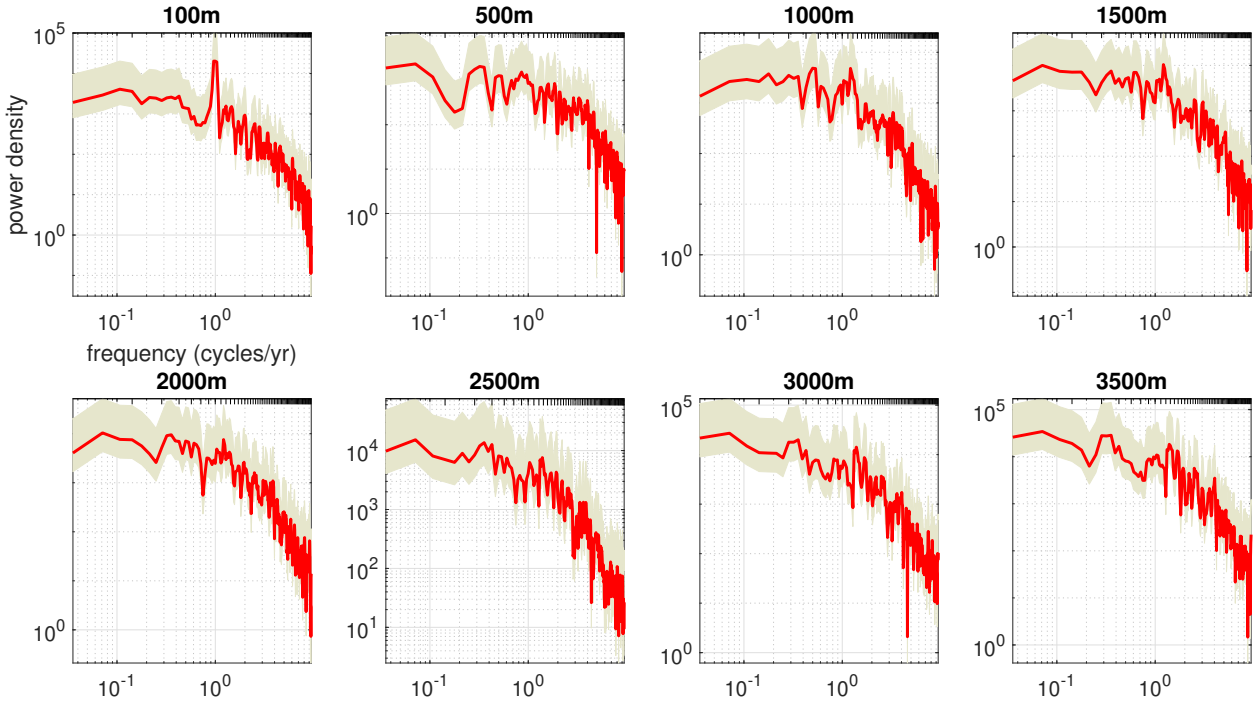

Figure 3.4: Power spectra for heave at many depths, calculated with Dual-DDW in the Hawaii Ocean Timeseries. Peaks at a frequency of 10^0 indicate seasonal variability. Tan shading indicates 95% confidence interval.

Figure 3.5 shows the power spectrum for the temporal empirical orthogonal function (EOF) corresponding to the first vertical mode of heave for HOT (Fig. 3.3c). In the same way that the first vertical mode explained 73% of the vertical heave variability in the HOT dataset, the first temporal EOF explains 73% of the temporal heave variability. Examining the power spectrum for this EOF can therefore summarize a significant portion of the temporal variability in heave from the HOT station. This power spectrum seems to have both high-frequency and low-frequency structure as expected. There is no peak at the seasonal frequency ($10^0 = 1$ cycle/yr), which is expected because the seasonal influence on heave in Hawaii is restricted to the surface ocean. The EOF represents the heave variability broadly across all depths, and would not capture this small part at the surface. Finally, there is a broad peak around 1 cycle/3 yr, which is likely related to ENSO.

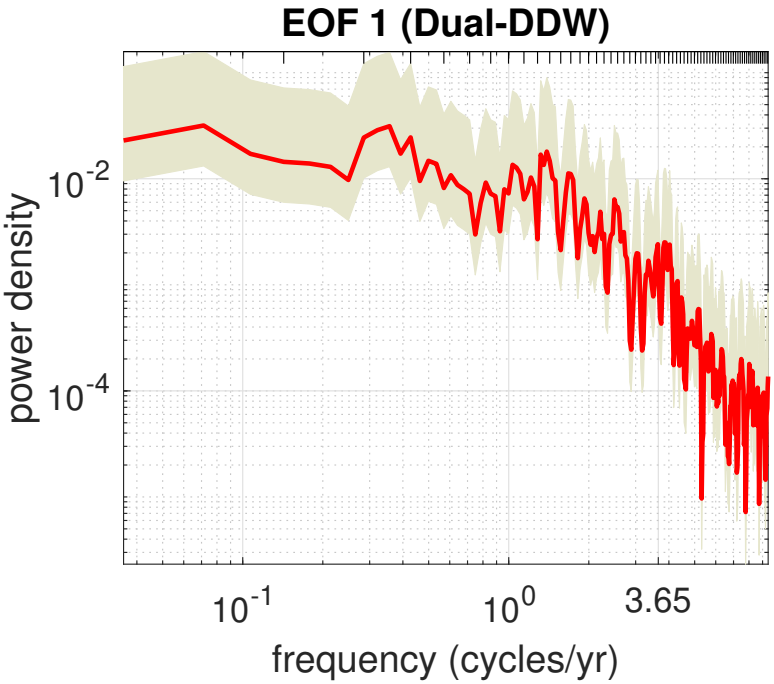

Figure 3.5: Power spectrum for the first EOF of heave calculated with Dual-Dynamic Depth Warping in the Hawaii Ocean Timeseries. A peak at a frequency of 10^0 indicates seasonal variability. A frequency of 3.65 indicates 100-day period variability. Tan shading indicates 95% confidence interval.

3.3.2 Bermuda Atlantic Time-series Study

In contrast to the HOT station heave, the Bermuda Atlantic Time-series Study (BATS) station heave looks very different depending on which method was used to calculate heave (Fig. 3.6). The density-based methods (conventional and warping) determine that heave is nearly constant for all depths, and this vertical pattern represents 61% of the heave variability. In contrast, Dual-Dynamic Depth Warping finds a vertical mode with a large increase in the amplitude of heave around 1500-2500m depth, and this mode explains about 58% of the heave variability calculated by Dual-DDW. Though these modes explain about the same percentage of variance in the BATS heave data, there is a stark discrepancy between the heave characterizations.

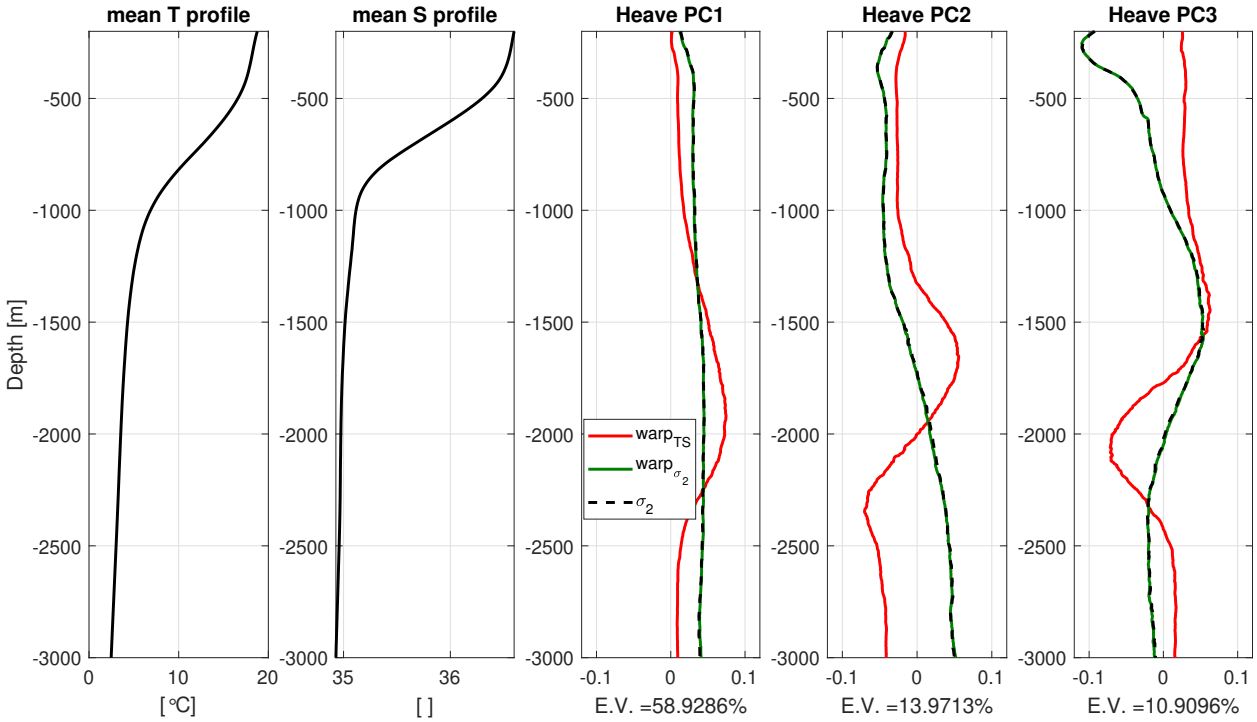

Figure 3.6: As Fig. 3.3, for the Bermuda Atlantic Time-series Study.

After examining specific examples in the BATS heave data, however, there is a logical explanation for this discrepancy. It is related to the high amount of lateral advection in the Sargasso Sea where BATS is located (*Michaels and Knap*, 1996). Figure 3.7 and 3.8 show an example of a measurement from BATS, where from approximately 2000-2500m depth, there is a large divergence between the heave estimates from the Dual-DDW method and the density warping method (Fig. 3.7a). The heave estimates from temperature and salinity are also shown, as the Dual-DDW method is a combination of these two techniques.

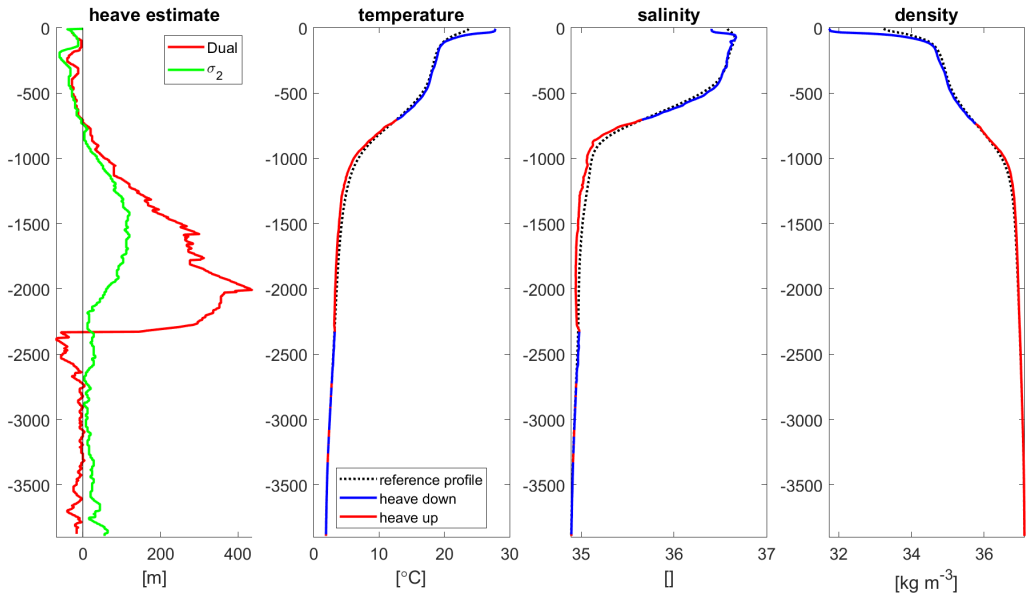

Figure 3.7: One CTD cast from the BATS dataset to demonstrate discrepancy between the density and temperature/salinity heave calculations. **a)** Heave estimates from Dual-DDW (red), density warping (green), temperature warping (black), and salinity warping (blue). **b)** Time-averaged temperature profile from BATS (reference profile; dotted line) and the sample temperature profile (solid line), with colors indicating which depths correspond to heave up (red) or down (blue) as calculated by Dual-DDW. **c)** As b), for salinity. **d)** As b) and c), but for potential density profiles, and the colors correspond to the heave as calculated by the density warping method.

Around 2300m depth, there is an abrupt jump in the temperature and salinity profiles (Fig. 3.8b,c). This cannot be explained by vertical movement; the water below would have had to heave up, and the water above would have had to heave down, which does not make physical sense. This jump is more likely due to the horizontal intrusion of a water mass with different temperature and salinity properties from the rest of the water column, which is a very different process from vertical heave. Luckily, our temperature and salinity-based warping methods can make this distinction. The temperature warping, salinity warping, and Dual-DDW methods all output a heave estimate that jumps from a large positive heave (300-1000m) to negative heave within one unit of depth change. We call this a failure because that massive jump in heave is nonphysical. The failure of those warping methods is an extremely useful feature; it distinguishes what can and cannot be explained by vertical heave.

In contrast, the potential density profile barely detects any kind of change, and simply interprets the entire segment of the profile as being heaved slightly upward (Fig. 3.8d). The density-based methods completely miss this change in temperature and salinity, because the reduction in density due to warming and the increase in density due to salinification compensate each other. Hence, the use of potential density is likely to misrepresent horizontal advection as vertical heave, or miss this variability completely. This example is typical of most of the BATS samples, and other samples have even more jumps in temperature and salinity due to horizontal advection. It is therefore especially important in this region to understand the influence of the horizontal movement of water in addition to vertical heave.

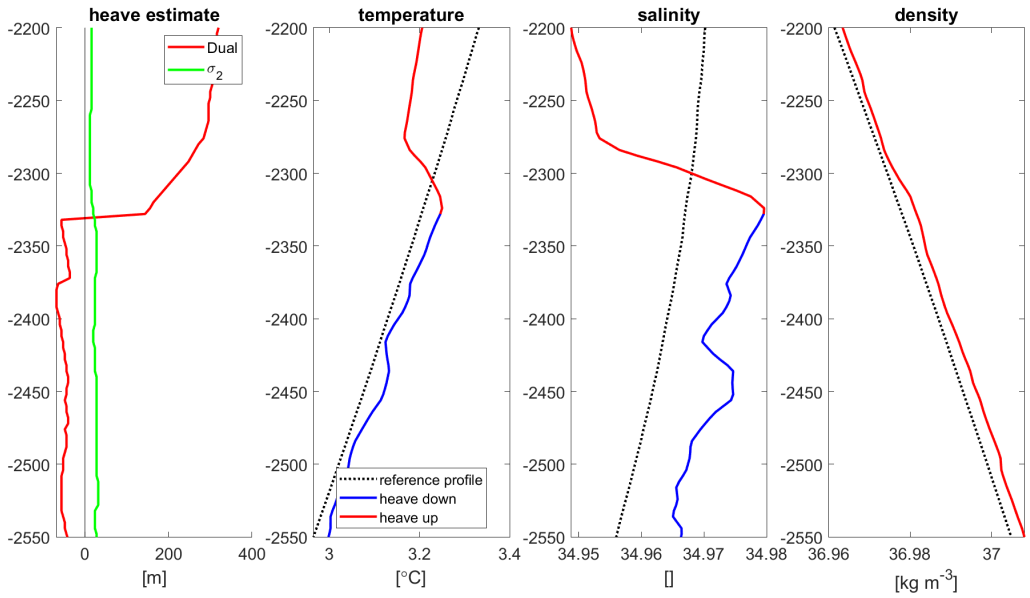

Figure 3.8: As Fig. 3.7, focusing on the depths where the warping methods fail. The abrupt changes in temperature and salinity cannot be explained by pure vertical heave, rather are likely indicative of horizontal advection.

The differences in how Dual-DDW and the two density methods handle horizontal advection in their heave calculations naturally causes differences in the heave power spectra. For all three methods, the power spectra remain nearly identical until 1500m depth. This depth is where the Dual-DDW method usually begins to detect small temperature and salinity changes due to horizontal movement of waters, and produces extremely large heave that is nonphysical. The effect of these failures can be observed in the power spectra for

the first EOF of heave derived from Dual-DDW and density warping (Fig. 3.9). The main difference between these spectra is that the density warping spectrum has a strong seasonal peak that is not pronounced for Dual-DDW heave. The density warping spectrum also has a broad peak around the 2-3 year period, which shifts toward 3-4 year period for Dual-DDW heave. There are also two peaks in the Dual-DDW spectrum around frequencies of 1.8 and 2.2 (equivalent to periods of 5.5 and 6.7 months) that are not present in the density warping spectrum.

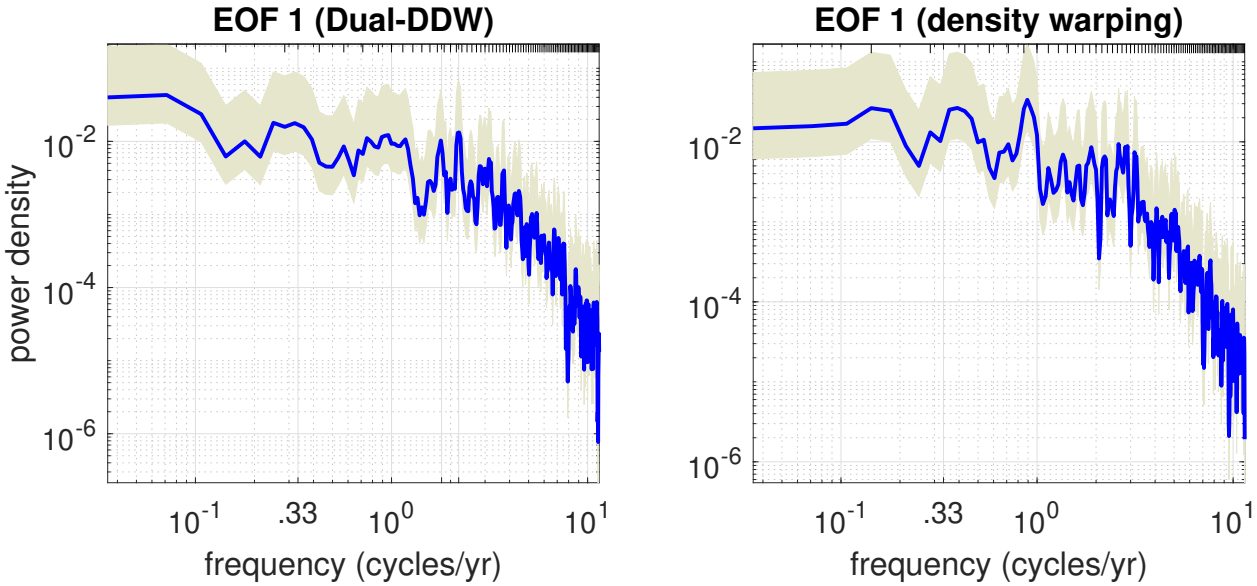

Figure 3.9: As Fig. 3.5, for the Bermuda Atlantic Time-series Study. Power spectra for the first EOF of heave calculated with Dual-Dynamic Depth Warping (left) and the density warping method (right). Tan shading indicates 95% confidence interval.

It is difficult to tell whether the spectra for either of these techniques represent the vertical heave that is actually occurring in this location. The structures present in the Dual-DDW spectrum may represent the periodicity of the horizontal intrusions into the BATS data, but it is hard to quantify how much of an effect this has on the spectra. The structures in the density warping may be broadly indicative of the heave in BATS because they do not detect the horizontal movement, or the heave may be incorrect. However, the upper 1000m of heave are approximately the same for all the heave estimation methods, so we can be more confident that the heave we calculated at these depths are indicative of the vertical heave in the BATS

region.

When we examine the spectra for several depths in BATS, we see several types of variability related to different processes that are known to occur in this region. First, we expect a seasonal cycle at the surface due to seasonal subduction of warm surface waters, which is displayed in Figure 3.10 as a very prominent peak in at 100m depth. We also see a broad peak near ENSO frequencies at 500m and 1000m depth, which may correspond to the ENSO-related mixing mentioned in *Michaels and Knap* (1996).

We also expect to see seasonal variability in the deep ocean at the BATS station, which is related to seasonal wind changes and deep water formation in the North Atlantic. The depth range of North Atlantic Deep Water in this basin is below 2000m. Indeed in the density-warping spectral diagrams for 2000-3500m depth, a seasonal peak appears, which may be indicative of this deep water formation process. However, it is still uncertain whether this variability is due to vertical heave or horizontal advection, or some combination of both, because the density warping method does not discriminate between the two. Further work is needed to understand the vertical and lateral contributions to variability in this region.

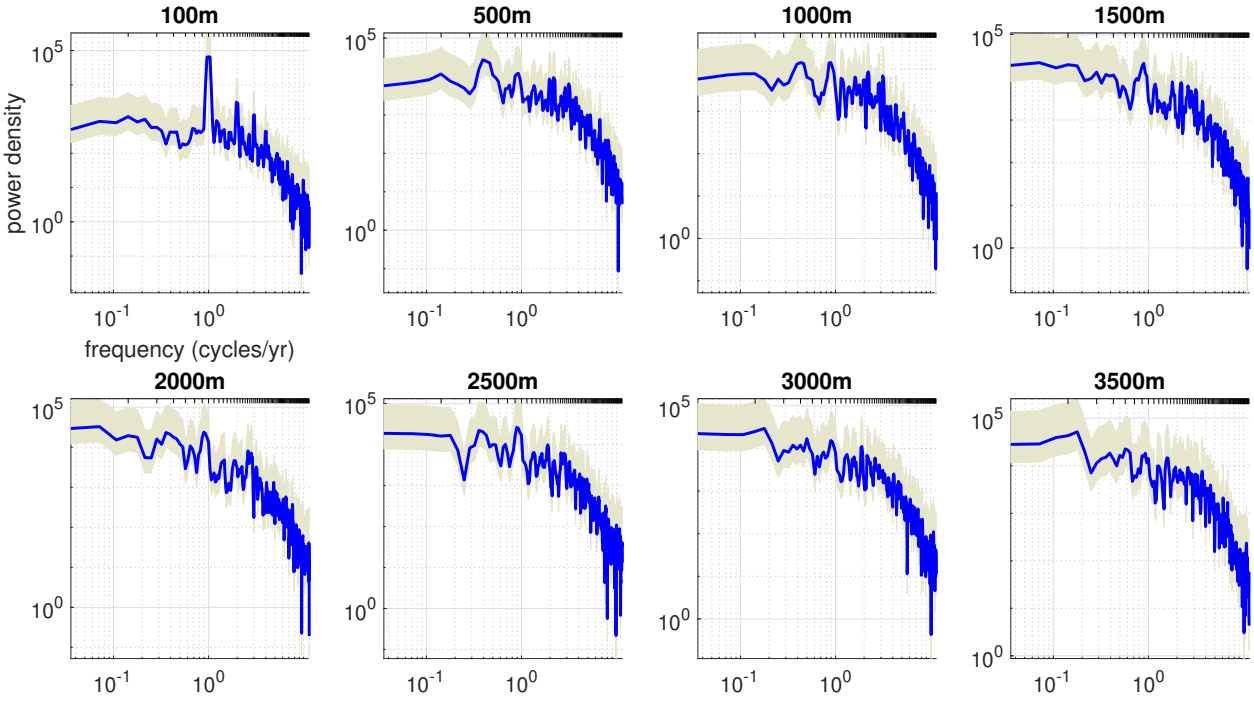

Figure 3.10: Power spectra for heave at many depths, calculated with density warping in the Bermuda Atlantic Time-Series. Peaks at a frequency of 10^0 indicate seasonal variability. Tan shading indicates 95% confidence interval.

3.4 Discussion

In applying our heave estimation methods to the HOT and BATS station data, we characterized the vertical and temporal variability throughout the entire depth of the ocean in these two locations. For both the HOT and BATS station data, the power spectra for heave make sense with both the local and larger-scale dynamics at play in each region. A surface seasonal cycle is clear in the upper 100m in both locations as expected, but more importantly we identified frequencies at depth that indicated teleconnections to other regions of the ocean thousands of kilometers away. Both locations contain ENSO periodicity; ENSO-related Rossby waves may cause heave in the deep ocean in HOT, while upper ocean mixing cycles that vary with ENSO are present in BATS. HOT and BATS are also both affected by changes in winds in the polar regions to form deep water masses that feed into the stations' ocean basins. For HOT, these are interannual (2-3 yr)

wind changes in the Southern Ocean where Pacific Deep Water forms. For BATS, there is a seasonal cycle at depth very likely to be related to the annual variability of North Atlantic Deep Water formation, which takes place near Greenland. Pacific Deep Water formation near Antarctica likely has a seasonal cycle as well, but it may not be as strong as the seasonal variability of North Atlantic Deep Water formation. Also, BATS is more likely than HOT to detect such a seasonal cycle, as BATS is much closer to Greenland than HOT is to Antarctica. Being able to detect these basin-scale processes at depth with our novel heave estimation methodology is very promising, and shows potential for extending our analysis to the global ocean.

There are likely to be some issues with expanding our analysis as-is near BATS. We found through the repeated failure of the Dual-Dynamic Depth Warping method in the BATS data that there is probably a signficant amount of horizontal advection in this region, and this variability would not be appropriately explained by pure vertical heave. Before attempting to expand our heave analysis across the North Atlantic, it would be optimal to first characterize these horizontal shifts, their timing, and their sources. It may help to modify our methodology by calculating heave in three dimensions to account for the lateral movement of isopycnals, as suggested in (*Durack and Wijffels*, 2010). Early reviews of the BATS program emphasized the need to address variability in the Sargasso Sea in three dimensions, to accurately capture the competing processes in the region (*Michaels and Knap*, 1996).

More recommendations for addressing these issues and applying our analysis to the North Atlantic are discussed in Future Directions in Chapter 6.

Chapter 4

Station vs. Argo Heave Comparison

After characterizing heave throughout the water column at two points in the ocean, we want to expand our analysis to a larger area of the global ocean by incorporating the Argo dataset. To determine whether the Argo data measure heave similarly to stations, we compare heave estimates between the station and the Argo profiles that were collected near the station.

We choose to focus only on the Hawaii Ocean Timeseries station (HOT) and the Argo profiles near Hawaii because there are many complications with the Bermuda station (BATS) and nearby Argo. As mentioned in the previous chapter, the region where BATS is located is prone to lateral mixing. Without a means to understand the horizontal variability in this region, it would not make sense to compare BATS and nearby Argo, which are more spread out and likely to be influenced by these various horizontal processes.

Even if we understood these horizontal processes, the comparison would be challenging because there is very little Argo data near the BATS station. Since 2004, there have been only 6 Argo profiles collected within 40 km of the BATS station and 25 profiles within 100 km, compared to 38 and 85 profiles within 40 km and 100 km of the HOT station. The low number of nearby profiles, especially within 40 km distance, makes it difficult to determine whether there is a correspondence between the BATS station and the Argo data. Argo floats farther from the station are more likely to experience high-frequency internal waves at different times than the station or that the station might miss altogether. This effect is especially problematic in the Sargasso Sea, where local, high-frequency processes are very common. This contributes to our decision to only evaluate the HOT station.

4.1 Methods

Our goal is to measure the correspondence between the heave estimates from the HOT station and nearby Argo floats. This is challenging because the Argo and the station are in different locations, and their samples were collected at different times.

To do this comparison, we restrict the Argo floats to only those within 50 km distance from the HOT station. We then compute heave using all three methods. We make sure to compute heave in the Argo data relative to the same profiles we used for the HOT data, i.e. the HOT mean temperature and salinity profiles, to ensure we are comparing against the same baseline for both datasets. Then for each Argo profile, we find the measurement from the HOT data that was collected the closest in time to the Argo measurement, and compute the difference in heave between those two measurements. We do this instead of interpolating the HOT data, because trying to increase the resolution of a monthly dataset may not be representative of what happened in this location, especially if there are internal waves propagating through the ocean here.

This outputs heave residuals between the Argo profile and the HOT profile as a function of depth. We repeat this for all the Argo profiles within 50km of the HOT station and evaluate the correspondence between the datasets.

4.2 Results

4.2.1 Vertical-Temporal Comparison

Despite being sampled in different locations and times, the match between the HOT station and nearby Argo seems to be quite good. At 400m depth, 59% of the Argo profiles have heave within 20m of that of the HOT station and 97% are within 50m. At 1400m depth, 41% of the Argo profiles have heave within 20m of that of the HOT station and 81% are within 50m. While the deep ocean heave match is not quite as good between the station and Argo, we expect heave to be larger at depth than near the surface based on the first principal component of heave in HOT (Fig. 3.3c), so we expect the residual of heave between the station and the Argo to increase with depth as well. For heave on the order of 100-150m at depth, being within

20-50m of the station heave is reasonable, especially since the collection locations are slightly different and the collection times can be very different.

The residual between the station and the Argo data can also depend on the temporal difference between the measurements, indicated by the size of the circles in Figure 4.1. The temporal differences between the Argo and station measurements range from less than one day to nearly six weeks; differences of multiple weeks can easily have a large effect on heave.

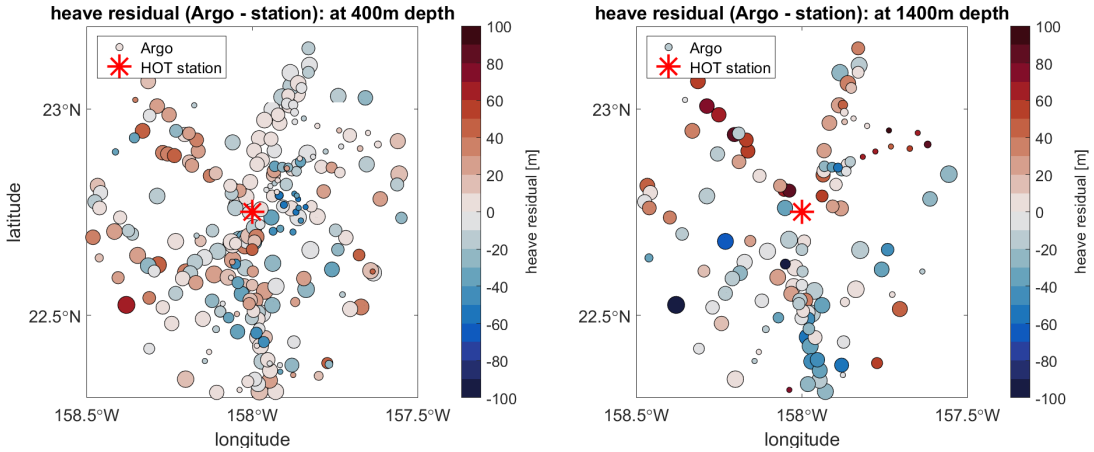

Figure 4.1: Map of the Hawaii station (red star) and the nearby Argo profile collection locations (circles). Circle color corresponds to the residual between heave calculated for that Argo profile and the HOT station at 400m depth [left] and 1400m depth [right]. Circle size indicates temporal correspondence; smaller circles indicate Argo profiles that were collected at very different times from the closest HOT measurement in time, can be up to 6 weeks. Heave generated by Dual-DDW.

For each of the three heave estimation methods (Dual-DDW, density warping, density conventional) we generate a plot like Figure 4.2, showing the heave calculated in HOT and Argo for many depths over time. From this, we can calculate the residual between each Argo profile and the closest temporal HOT profile (Fig. 4.3).

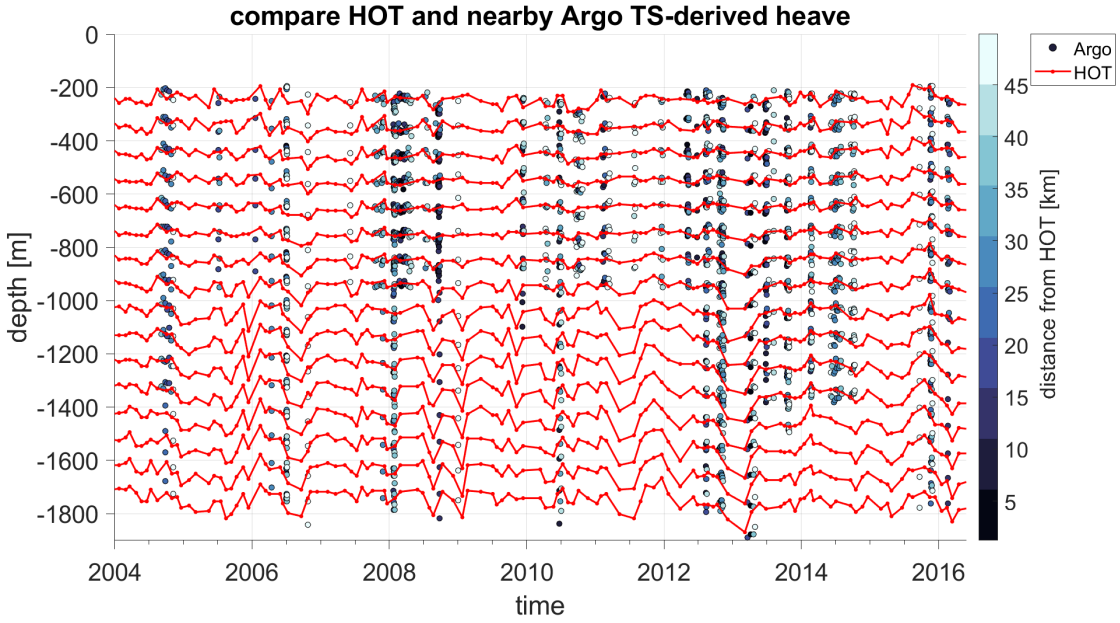

Figure 4.2: Heave at several depths generated by Dual-Dynamic Depth Warping in the HOT station (red line) and nearby Argo measurements (blue dots). Shade of blue for Argo indicates the distance between the HOT station and the Argo measurement in kilometers.

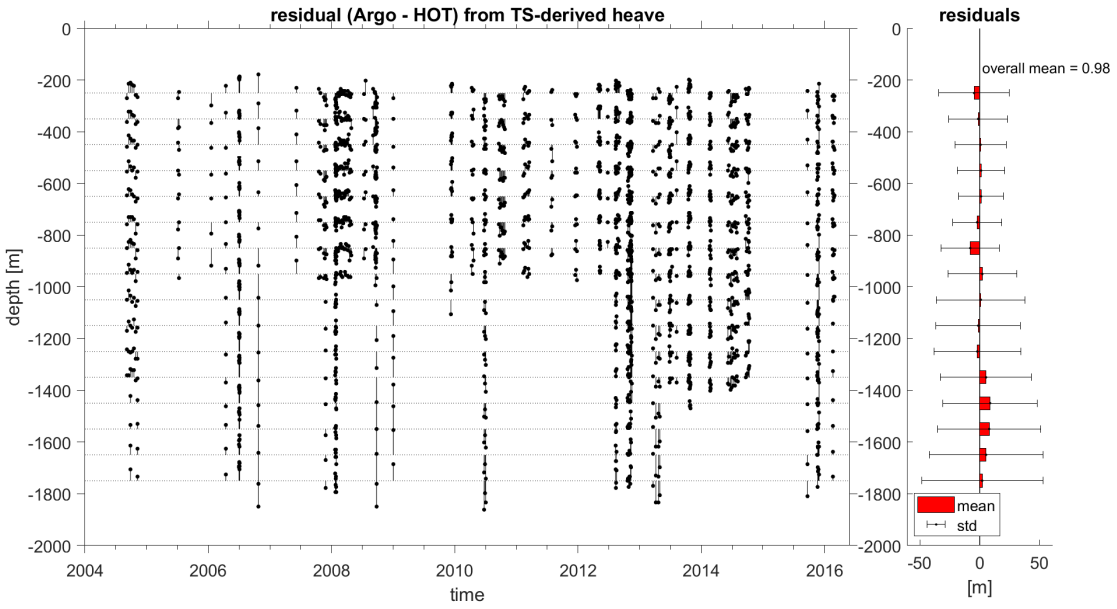

Figure 4.3: [Left] Residuals between the HOT station and nearby Argo heave. [Right] The mean and standard deviation of heave for each depth level. Heave generated by Dual-Dynamic Depth Warping.

Looking at the mean and standard deviation of the residuals taken over time for many depths, the choice of heave estimation method makes very little difference (Fig. 4.4). The mean of the residuals for each method is very close to zero for all depths, which should be the case for averaging across many Argo profiles, so there does not appear to be a systematic bias in heave for any of the methods. There is a large increase in the standard deviation below 1000m depth, however, and this is likely due to a large decrease in sample size since less than half of the Argo profiles near Hawaii reach past 1000m.

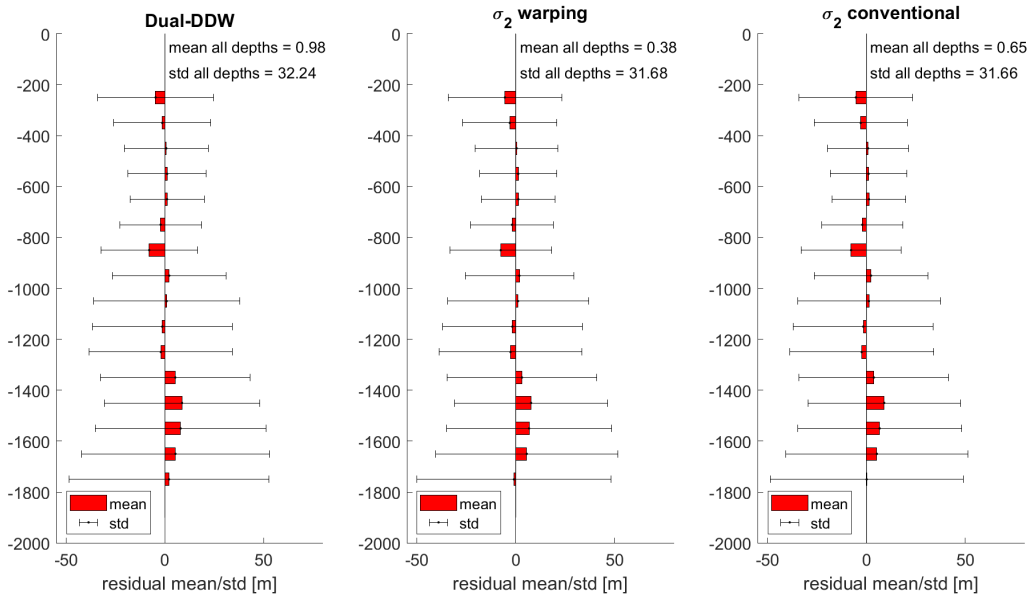

Figure 4.4: Difference between heave calculated at the HOT station and Argo near Hawaii, as a function of depth (Argo heave minus HOT heave). [Left] Heave calculated by Dual-DDW. [Center] Heave calculated by density warping. [Right] Heave calculated by the conventional potential density method. "Mean all depths" is the mean of the red bars for the entire water column, and "std all depths" is the mean standard deviation across all depths.

Though the differences between the methods are small, the residuals between HOT and Argo calculated by the Dual-DDW method have a slightly larger standard deviation than those calculated by the density-based methods. This is likely because the Dual-DDW method produces more variable heave than the other methods (Fig. 4.5). In the depth range of the Argo data, the heave calculated by Dual-DDW usually has a greater standard deviation than the heave calculated by the density-based methods, in both the HOT station and the nearby Argo. If the heave estimates are more variable to begin with, the residuals between HOT and Argo will also be expected to have greater variance. This could imply that the Dual-DDW method is noisier than the other methods, though Dual-DDW calculates less variable heave than the other two methods in the deep ocean in HOT (below 2500m depth) (Fig. 4.5a). The contributions of temperature and salinity may help Dual-DDW explain more heave. We recommend further quantifying the noisiness of the Dual-DDW method as a direction for future study. At least near the HOT station, however, this difference in variance

does not seem to make a significant difference in the residuals between the three heave estimation methods.

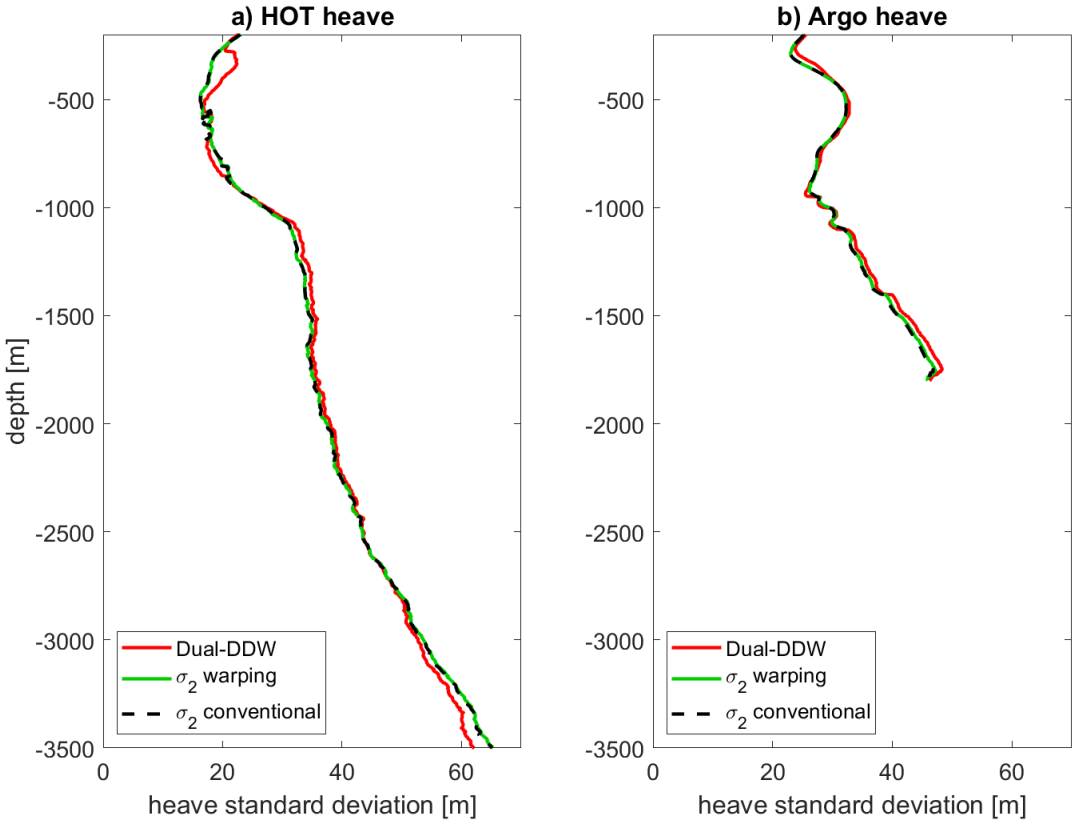

Figure 4.5: Standard deviation of heave as a function of depth, in a) the Hawaii Ocean Timeseries (HOT) data and b) the Argo data near the HOT station. Lines indicate the heave calculation method: Dual-DDW (red), density warping (green), and the conventional density method (black dashed). The depth range for Argo is less than that of HOT, and therefore does not extend to depth.

4.2.2 Distance-Dependent Correlation

We also measure the correlation between the Argo float heave and the station heave as a function of distance (Fig. 4.6). We do this by expanding the distance threshold for accepting Argo profiles by 5 km at a time and computing the heave correlation between the station and the incrementally expanded Argo dataset. There should be a gradual decrease in correlation with distance just from adding more data points (Fig. 4.7), but the drop in correlation between 30-70km distance is sharper, especially below 1000m depth. This indicates

a real distance-dependence.

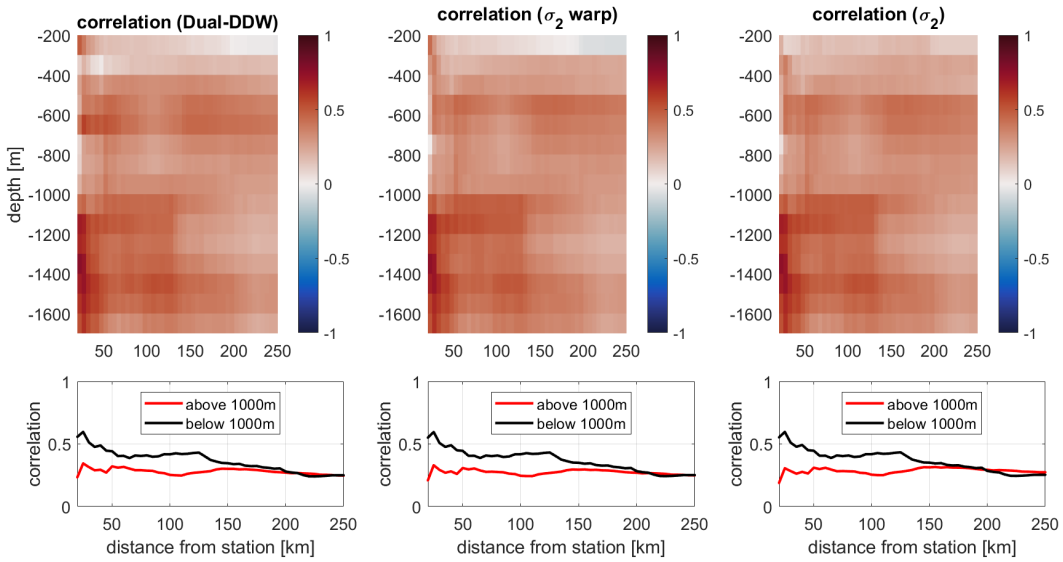

Figure 4.6: Correlation between the HOT station and Argo heave as a function of distance, with heave estimated by [left] Dual-Dynamic Depth Warping, [center] density warping, and [right] the conventional method. [Top row] Correlation as a function of distance and depth. [Bottom row] Correlation as a function of distance, with the mean for 200-1000m (red line) and the mean for 1000-1700m (black line).

The correlation as a function of distance and depth was nearly identical for all three methods, but Dual-DDW seemed to produce slightly higher correlation at mid-depths (400-600m) compared to the other heave estimation methods. This could be related to the reversal of the salinity profile in this region, which occurs near these depths. Our hypothesis is that because the Dual-DDW method takes into account the shape of the entire temperature profile and the entire salinity profile, the Dual-DDW method can use extra information from the relatively complex structure of the salinity profile to calculate heave more consistently. The performance of Dual-DDW compared to the density-based methods in non-monotonic environments warrants further study.

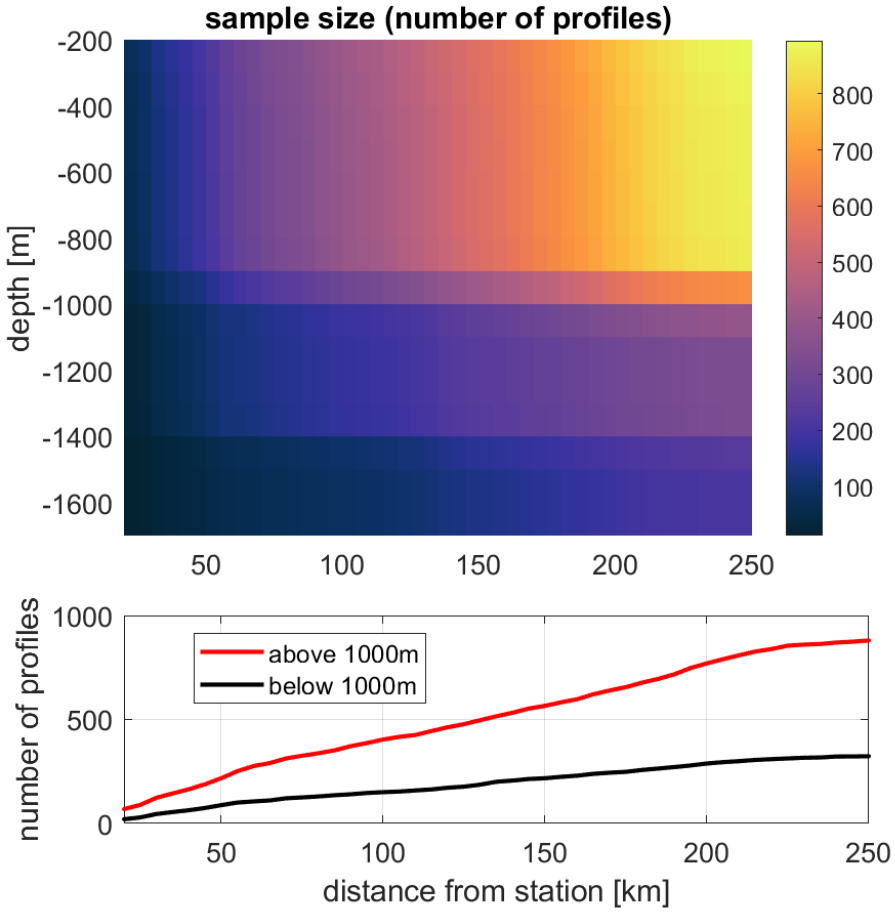

Figure 4.7: [Top] Number of Argo profiles as a function of distance and depth. [Bottom row] Number of Argo profiles as a function of distance, with the mean for 200-1000m (red line) and the mean for 1000-1700m (black line).

4.3 Discussion

This is the first time the Hawaii Ocean Timeseries has been compared to nearby Argo data. Overall the match between Argo and HOT seems reasonable for all three heave calculation methods. The residuals between the station and Argo heave had no systematic biases with depth, and the magnitude of the residuals was reasonable for the most part. The match also depended on distance, supporting the idea that Argo

floats farther from the station are subject to high-frequency changes, such as internal wave activity, which can alter their estimates of heave. There were some slight differences between the heave estimation methods in the distance correlations that may imply the methods respond differently to different shapes of ocean profiles. Future work should test a wider variety of ocean profiles and heave to better quantify the ability of the Dual-DDW method to capture heave variability compared to the two density-based methods.

The match between these independent datasets seems reasonable, but this is only one point in the ocean. It may be helpful to investigate the correspondence between Argo and another stationary dataset in this region, such as the TAO array in the Equatorial Pacific. *Desbruyères et al.* (2017) found that the best correspondence between ship hydrography and Argo data was in the North Pacific basin, so it would be interesting to conduct a similar analysis with the Bermuda station and nearby Argo after accounting for horizontal variability, to see whether the correspondence is worse in the Atlantic.

Chapter 5

Spatial Patterns of Heave in North Pacific Argo

Having shown reasonable agreement between heave estimates from the Hawaii Ocean Timeseries and nearby Argo floats, there is significant potential for our analysis to extend to the Argo array in the rest of the North Pacific Ocean. We focus our analysis on the Argo data in the North Pacific for three reasons: (1) we showed correspondence between station and Argo heave near Hawaii, which is located in the center of this basin; (2) the North Pacific is the widest basin with the least complicated topography out of all the ocean basins on Earth, thus making it ideal for tracking the unobstructed, large-scale propagation of waves; (3) the Equatorial Pacific is likely to have coherent variability associated with the El Niño Southern Oscillation (ENSO). In this preliminary analysis, we use our novel method, Dual-Dynamic Depth Warping, to compute heave in the Argo data for the entire North Pacific Ocean. We then use this heave data to characterize both natural and climatic changes in the North Pacific.

5.1 Argo Data Product

The Argo data used in this study are interpolated to standard depth levels, which results in the depth resolution ranging from 10-100m (*Argo*, 2000; *Forget*, 2016). This is because these data were used to constrain the ocean state estimate in a climate model, ECCO version 4, and were thus depth-interpolated onto the ECCO grid (*Forget et al.*, 2015). In line with our synthetic tests and the rest of our previous analysis, we linearly interpolated the Argo data to 4m depth resolution.

5.2 Methods

5.2.1 Argo Data Analysis

Characterizing the variability of heave was relatively simple in the HOT and BATS datasets because those data were collected from a single geographic point. In contrast, the Argo data in the North Pacific contains hundreds of thousands of ocean profiles collected sporadically in time and space across an entire ocean basin. We therefore use some compression techniques and averaging to characterize the spatial variability of heave in Argo.

We group the Argo floats into 4x4-degree boxes and treat each box as an individual dataset of profiles collected from the same location. We then apply Dual-Dynamic Depth Warping to each Argo float individually relative to the mean profile in each grid box, and average the heave within each grid box at each depth and time interval (every month from 2007-2016). We intentionally select a similar temporal resolution to the HOT data for the sake of comparison. This approach allows us to calculate heave for individual profiles while reducing the size of the dataset to observe broader patterns of variability. We use these 4x4-degree boxes for the rest of the Argo analysis, and there are approximately 500 of these boxes in total in the North Pacific Ocean. We also restrict our analysis to the boxes with over 50% temporal coverage and a maximum time interval without data of 1 year or less.

After calculating heave and binning the heave data in Argo, we only use the heave data between 40m-1850m depth rather than the full Argo range of 0-2000m. At the very surface, Dual-DDW often fails (i.e. produces very large heave values) because the surface ocean has large temperature and salinity changes that are not indicative of vertical heave. At depth, many heave profiles are automatically cut off above 2000m depth; if a profile experiences 150m of upward heave at 2000m depth, the heave profile ends at 1850m since there is no more data below 2000m to fill in the rest of the heave profile. Since heave at 2000m depth is typically on the order of 100-150m, we only examine heave data down to 1850m depth.

5.2.2 Hawaii Station vs. North Pacific Argo

Our first test in determining whether we can reliably use heave from the Argo data to study oceanic processes is to look at the structure of the heave relative to a single reference point, the Hawaii Ocean Timeseries (HOT) station. Our approach is similar to what we used in Chapter 4, when we calculated the residual between the heave estimates from the HOT station and nearby Argo. In this analysis, rather than the Argo data being treated as individual profiles, the data is binned into 4x4-degree boxes and 1-month temporal resolution. Therefore, comparing the Argo data to the HOT measurement closest in time to the Argo temporal bin would not be appropriate. We instead interpolate the HOT data temporally to match the Argo data, then compute the heave residual by subtracting the HOT heave from the Argo heave in each geographic bin at many depths.

5.2.3 Linear Model

To study various oceanic processes in the North Pacific Argo data, we fit a linear model to the heave data. Our model consists of three predictors corresponding to processes we expect to be detectable in the North Pacific Ocean. The first predictor is the heave trend measured over the period of 2007-2016, which indicates gradual changes in heat content that are likely related to climate change. The second predictor is the El Niño Southern Oscillation (ENSO). ENSO is an irregular, naturally-occurring phenomenon that has a large impact on the global climate. We use the Nino 3.4 index to represent ENSO variability (*Rayner et al.*, 2003). The third predictor is the seasonal cycle, which corresponds to natural changes in solar radiation at the Earth's surface and can cause changes in winds and ocean properties. Seasonality is also associated with waves that propagate through the ocean in different ways. To ensure that our model captures all the phases of the seasonal cycle, we use two phases of the seasonal cycle that are offset by 90 degrees.

Our model is as follows:

$$H = \beta_0 + \beta_T X_T + \beta_{ENSO} X_{ENSO} + \beta_{S_1} X_{S_1} + \beta_{S_2} X_{S_2}$$

where H is heave, β_0 is an intercept term, $\beta_T X_T$ is the trend component, $\beta_{ENSO} X_{ENSO}$ is the ENSO (Nino 3.4) component, and the seasonal component is composed of the two terms $\beta_{S_1} X_{S_1}$ and $\beta_{S_2} X_{S_2}$

representing the sine phase and cosine phase of the seasonal cycle, respectively. These two phases of the seasonal cycle are separate terms in our model, but the sum of their slopes form an overall slope representing the association between heave and seasonality, $\beta_S = \beta_{S_1} + \beta_{S_2}$.

The ENSO and seasonal components are normalized to unit variance such that the slopes β_{ENSO} and β_S are expressed in meters of heave per unit variance. The trend, β_T, is expressed in meters of heave per year. More terms could be included in this model, but we choose to keep the model simple to avoid overfitting and to investigate the Argo heave data's ability to characterize large-scale processes.

5.2.4 Multi-Taper Coherence Analysis

Multi-taper coherence analysis is used to compare two timeseries at several frequencies. It also calculates phase offsets between timeseries, which helps to measure the propagation of periodic processes. Applying this analysis to heave in Argo is useful because this analysis can detect coherent wave processes across different locations, even if those locations experience the phases of the wave differently.

In the Argo data, we selected a depth level and calculated coherence between the heave from a chosen reference grid box and every other grid box at that depth. We repeated this for several depths and frequencies, and examined the phase offsets in coherent regions to look for propagating waves. Coherence analysis goes one step beyond the capabilities of the linear model, which can only show correlations between heave and ocean processes. Coherence allows us to not only identify geographic regions where a periodic process is present, but also to visualize propagating waves in these regions through phase offsets.

5.3 Results

5.3.1 Hawaii Station vs. North Pacific Argo

We first compare the heave estimates in the North Pacific Argo data and the Hawaii Ocean Timeseries (HOT) station, to determine whether our Argo heave calculations are consistent with the expected variability and mean state in the North Pacific (Fig. 5.1).

The variance of the residual between the Argo and HOT heave estimates increases with distance away

from the HOT station, which is expected because regions that are farther from the HOT station are more likely to experience different atmospheric and oceanic influences than the HOT station. There are especially large increases in the variance of the residual in regions where eddies often form, particularly in the Kuroshio Current near Japan and near the Equator (*Katsumata*, 2016). Eddies produce localized, dramatic variations in heave, so it makes sense that regions with large eddy activity have a highly variable heave residual with the HOT station. The enhanced variance near the Equator disappears around 800m depth, but the variance near the Kuroshio Current persists to at least 1850m, indicating how strong eddy activity in this western boundary current can influence the deep interior ocean.

The mean heave offset between Argo and HOT also matches the structure of ocean circulation in the North Pacific (Fig. 5.1). This time-averaged heave offset can be used to calculate the mean slope of isopycnals in the North Pacific. Since we define positive heave to be upward, a positive mean heave residual relative to the HOT station indicates the isopycnals in that region are shallower on average than the isopycnals near Hawaii; shallower isopycnals usually correspond to colder temperature profiles, therefore we show positive heave residuals in blue. The converse is true for a negative mean heave residual, which corresponds to deeper isopycnals and typically warmer water. The lower plot in Figure 5.1 clearly shows the structure of the North Pacific Gyre at 500m depth, which is influenced by the warm, northward-flowing Kuroshio Current on the western boundary and the eastward-flowing Kuroshio Extension, and the cold return flow of the California Current on the eastern boundary (*Reid*, 1997). The mean heave residual between HOT and Argo from 1000-1800m depth also seems to reflect the weaker and more complex circulation in the deep North Pacific.

We thus know that the estimates of heave in the North Pacific Argo from Dual-Dynamic Depth Warping produce the large-scale structures of heave that we expect. Having established the basic structures of heave in the North Pacific, we can continue our analysis to study more complex large-scale processes.

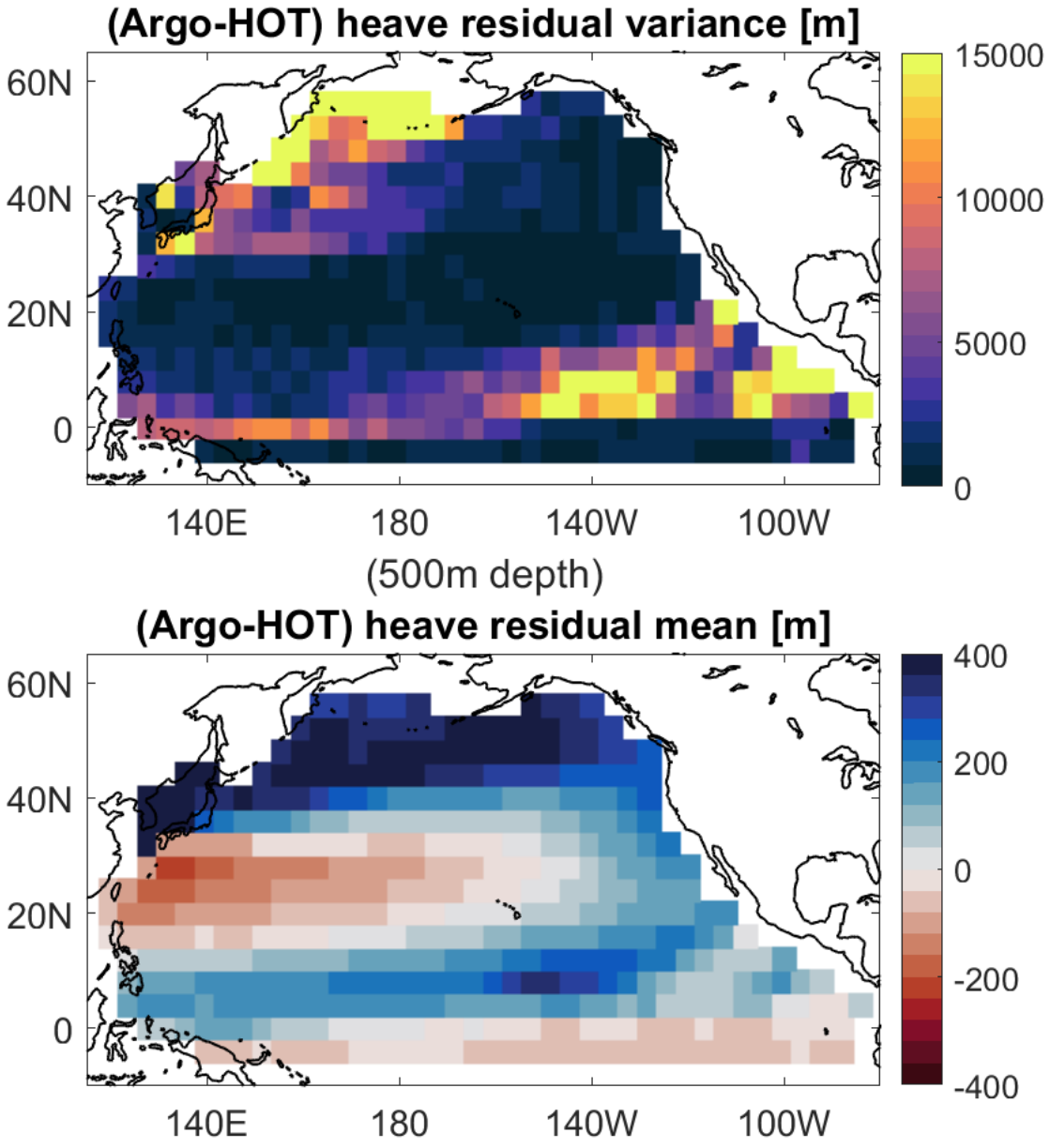

Figure 5.1: Heave residual between the North Pacific Argo data and the Hawaii Ocean Timeseries (HOT) station variance (top) and mean (bottom), at 500m depth.
Positive mean heave residual (blue) represents regions with shallower isopycnals on average compared to the HOT station, which typically corresponds to colder water. Negative mean heave residual (red) indicates deeper isopycnals and typically corresponds to warmer water compared to the HOT station.

5.3.2 Linear Model

Using our linear model for heave, we quantify seasonal variability, the El Niño Southern Oscillation (ENSO), and heave trends in the North Pacific. We study the vertical structure of these variables by regressing them onto heave at many depths. We also identify some local changes using additional coherence analysis.

Considering that heave data can be quite noisy, the model fit is quite good in general, and seasonal variability has the largest association with heave on average in the upper 200m of the North Pacific Ocean. However, the model fit decreases with depth. This could be due to the greater magnitude of heave at depth, which could increase the magnitude of noise in the heave data. The worse fit at depth may also be related to the reduction in data coverage below 1000m depth, which could cause the data to be noisier. Additionally, considering that seasonality and ENSO tend to occur largely in the surface ocean, it is reasonable that the fit of our model generally decreases with depth.

The model fit and expression of each component of the model also varies greatly with location. In this section we discuss both small and large-scale variations in the contributions of seasonality, ENSO, and trends to heave in the North Pacific Argo data.

Changes in the Kuroshio Current

The first result from our linear model is a distinct feature off the coast of Japan between 140-340m depth (Fig. 5.2). There is a strong positive heave trend at 28°N, and a strong negative heave trend at 32°N. The magnitude of these opposing heave trends relative to the surrounding regions and the way the trends extend eastward imply they represent changes in the Kuroshio Current. The Kuroshio Current transports warm water from the equatorial regions to the mid-latitudes, and is therefore associated with negative heave on average (The negative heave of the Kuroshio can also be seen in the mean heave state in Figure 5.1). A positive heave trend in the south and a negative heave trend in the north implies that the Kuroshio Current is shifting northward during 2007-2016.

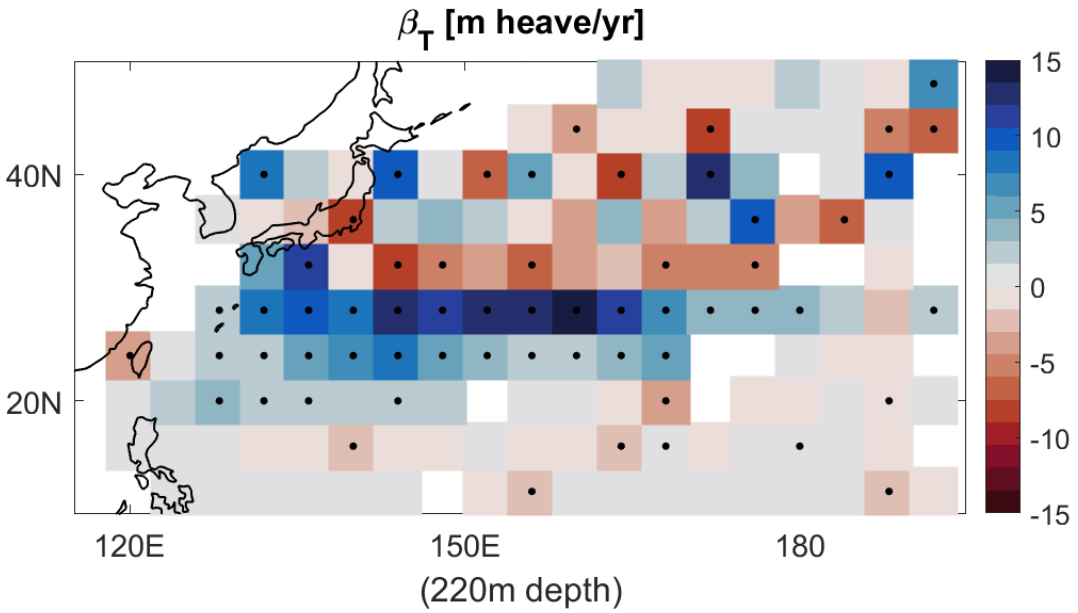

Figure 5.2: Heave trend in m yr^{-1} in the region of the Kuroshio Current, calculated by our linear model for the time period 2007-2016. Black dots indicate locations where the trend was significant at the 95% confidence level. Shift in the Kuroshio Current indicated by the large meridional heave gradient near (32N,145E).

However, our heave calculations also suggest that the Kuroshio Current responds to ENSO and seasonal variability, which is consistent with previous findings (*Qiu and Lukas*, 1996). The ENSO signal is present in the Kuroshio region from 140-240m depth, indicating that ENSO may influence the position of the Kuroshio Current (Fig. 5.3). The association between heave and ENSO is the opposite sign of the heave trends in this region. Additionally, the heave trends and ENSO variability in the Kuroshio are overlain by strong seasonal variability (Fig. 5.4). The seasonal association with heave is about three times greater in magnitude than the other components of the model in this region, and is present from the surface to 280m depth.

The case of the Kuroshio Current is a good example of how our linear model can reveal the contributions of climatic and natural processes to heave, even when their contributions are opposing signs, varying magnitudes, and occur on different timescales. Also, being able to view changes at the relatively small spatial scale of an individual current indicates the potential to use this approach for detailed heave analysis in Argo.

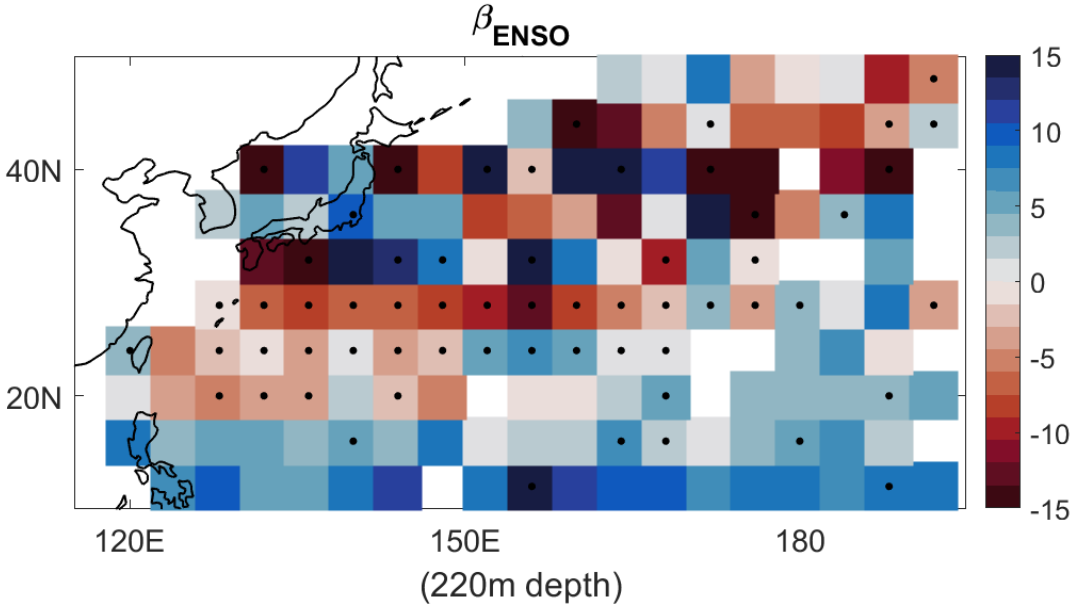

Figure 5.3: Heave associated with the El Niño-Southern Oscillation in m heave/unit variance in the region of the Kuroshio Current, calculated by our linear model. Black dots indicate locations where the association was significant at the 95% confidence level.

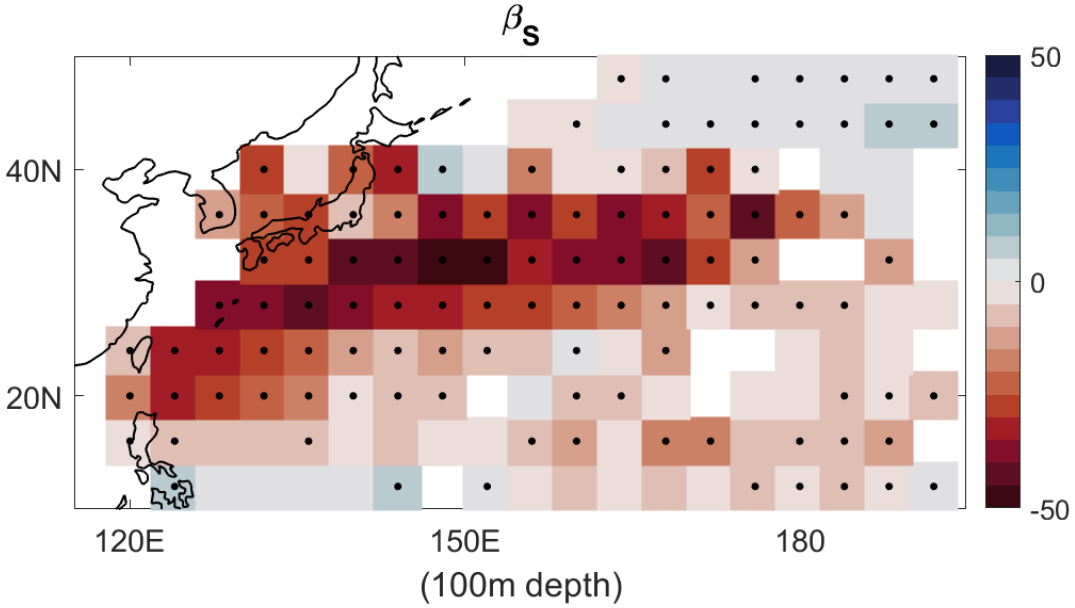

Figure 5.4: As Fig. 5.3, for heave associated with seasonal variability in m heave/unit variance.

El Niño-Southern Oscillation and Coherence Analysis

Our linear model results show that ENSO has a strong correlation with heave in the North Pacific, especially in the surface ocean. At 60m depth, there seem to be two regions in the North Pacific that respond to ENSO in opposite ways (Fig. 5.5). On the Equator from 150E to 90W, a unit variance increase in ENSO (i.e. an increase in the Nino 3.4 index, indicating a shift towards the El Niño phase of the oscillation) is associated with about 10-20 meters of downward heave, or warming. The eastern boundary of the North Pacific seems to respond to ENSO in a similar way. In the western Pacific, a unit variance increase in ENSO is associated with about 5-15 meters of upward heave, or cooling.

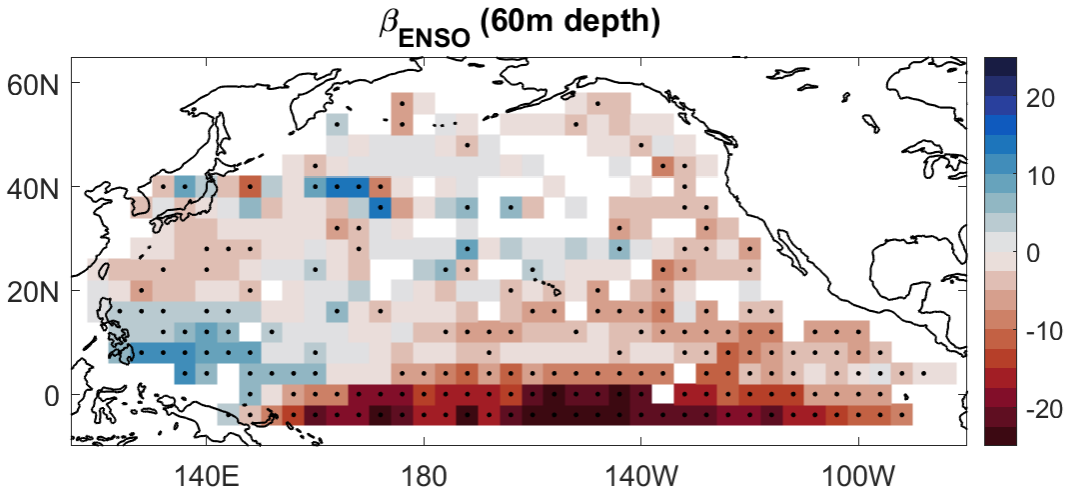

Figure 5.5: The slope for the El Niño-Southern Oscillation component of the heave model at 60m depth. Slope is expressed in meters of heave per unit variance in the Nino 3.4 index. Black dots indicate locations where the ENSO component of the model was significant at the 95% confidence level.

Coherence analysis reveals that these are two coherent regions that experience ENSO in opposite phases (Fig. 5.6). Coherence analysis identifies the Equator and eastern boundary of the North Pacific as experiencing ENSO variability together (Fig. 5.6a), and the western Pacific experiencing ENSO at a 180-degree lag behind the equatorial region (Fig. 5.6b). It seems that the coherence calculation reveals more of the ENSO pattern is coherent than can be identified using correlation in the linear model. Coherence analysis therefore seems to provide a more complete description of the ENSO-related heave variability in the North Pacific.

The downside to coherence analysis is that it calculates coherence for a single frequency. For studying an irregular phenomenon such as ENSO, this may cause problems. Using coherence also does not provide a framework for studying multiple processes at once, making it difficult to attribute heave variability to individual processes. At 60m depth in the North Pacific we assumed that the coherence at 3-yr period variability was associated with ENSO because our linear model showed a dominant ENSO signal at this depth, but without the linear model it would be difficult to tell if that coherence was purely related to ENSO. For the rest of our analysis, we continue to use the linear model because it is a simple way to partition heave into contributions from seasonality, ENSO, and trends.

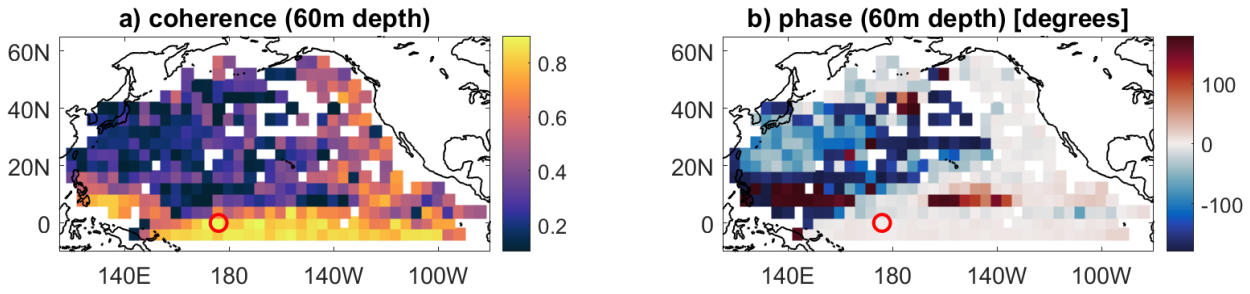

Figure 5.6: (a) Coherence and (b) phase offset at a frequency of 1 cycle/3 yr at 60m depth. Coherence was calculated between the reference location (0N,176E) (red circle) and every other location in the North Pacific Argo data. A positive phase offset indicates that location experienced variability after the reference location.

Coherent Equatorial Wave Patterns

Though coherence analysis has some limitations, when used in addition to a linear model it helps us visualize wave processes and determine their causes. For the Argo heave data in the Equatorial Pacific, coherence analysis finds coherent heave patterns at 1000m depth (Fig. 5.7a). This coherence is present for variability with periods ranging from 6 months to 4.5 years. There are also clear, gradual phase offsets along the Equator for all of these frequencies (Fig. 5.7b).

These propagating equatorial waves could be related to ENSO, seasonal variability, or many other types of variability. Seasonal variability is a particularly likely candidate because preliminary examination of our model results show zonal gradients in heave on seasonal timescales at depth along the Equator. These results indicate that coherence analysis could be helpful for studying heave phase offsets in further detail. Ultimately, using a wave view in addition to a linear model could be a more complete approach for describing heave in the North Pacific than using a linear model alone.

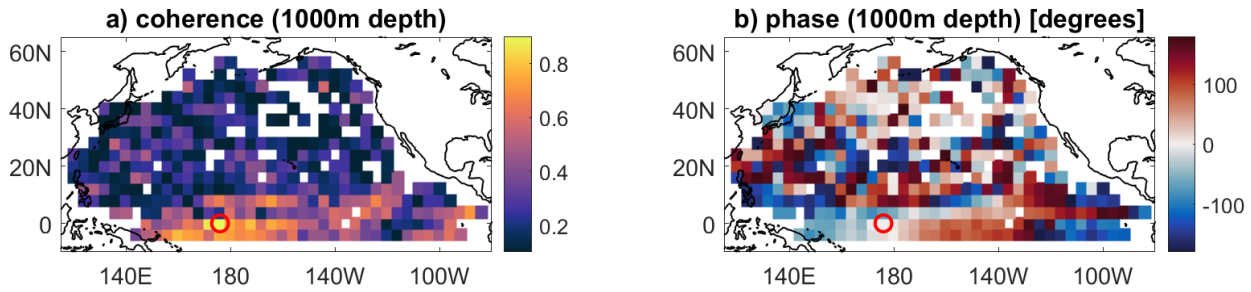

Figure 5.7: (a) Coherence and (b) phase offset at a frequency of 1 cycle/3 yr at 1000m depth. Coherence was calculated between the reference location (0N,176E) (red circle) and every other location in the North Pacific Argo data. A positive phase offset indicates that location experienced variability after the reference location.

General Structures of Natural and Climatic Variability

The results from our linear model for heave are highly variable with location and depth, and often have competing relationships with heave. Understanding the general structures of seasonal variability, ENSO, and heave trends in the North Pacific is important for determining their influence on ocean measurements and quantifying changes in the ocean. Though further analysis is required to understand these results in detail, here we present some initial descriptions of the spatial variability of these three processes.

In the upper 100m of the ocean, seasonal variability is the largest contributor to heave on average in the North Pacific. This corresponds to the seasonal subduction of warm surface waters, as discussed in *Bindoff and McDougall* (1994). The seasonal heave signal is particularly strong at mid- to high-latitudes. Below the surface ocean, seasonal variability is more heterogeneous and is mostly restricted to regions south of 20°N. From 100-300m depth, the West Equatorial Pacific has an inverse relationship with the seasonal cycle while the East Equatorial Pacific maintains a positive correlation with the seasonal cycle. The phase relationship between heave and seasonal variability also seems to change with depth. This may indicate the propagation of waves across the Equator. Further investigation of these phase changes can provide additional insight into deep Equatorial Pacific variability.

ENSO also explains a large portion of the heave variability in the Equatorial Pacific. The spatial structure of ENSO-related heave changes dramatically with depth. In the surface ocean the entire equatorial region experiences negative heave (warming) in the positive phase of ENSO, but at mid-depths the relationship

between ENSO and heave in West Equatorial Pacific changes, and the region instead experiences upward heave during El Niño. This is probably indicative of the shallowing of the zonal isopycnal slope that occurs along the Equator during El Niño events. This zonal gradient along the Equator persists to about 1500m depth along the eastern and western margins in the Equatorial Pacific. Some ENSO-related heave variability persists to 1850m depth in the central Pacific near (8N,170W), but this is a localized phenomenon.

Heave trends in the North Pacific are smaller in magnitude than the seasonal and ENSO-related heave on average, but the trends are what we are most interested in for quantifying ocean heat uptake. Downward heave trends associated with gradual warming dominate at high latitudes; the heave trend is strongest at the surface, but persists to 1850m depth. There are some regions at mid-latitudes that experience gradual cooling. The region containing the Kuroshio Current has the most dramatic heave trends in the North Pacific, but this region is influenced by ENSO and seasonal variability as well.

Overall it seems that partitioning heave into seasonal, ENSO, and trend components is useful, and digging deeper into the regional variability of these processes can help us understand these processes' influence on heave in the North Pacific.

5.3.3 Linear Model Regional Variations

To better characterize seasonal variations, ENSO, and heave trends in the North Pacific, we identify three coherent regions to study in further detail (Fig. 5.8). The first region is the East Equatorial Pacific (EEP), located between 4°S to 12°N and 140°W to 80°W. The second region is the West Equatorial Pacific (WEP), located from 4°S to 4°N and 120°E to 180°E. The third region is the High-Latitude North Pacific (HLNP), ranging from 36°N to 56°N and 140°E to 128°W.

We select these three regions mainly because they seem to express different components of the model; the EEP has a strong ENSO signal, the WEP has strong seasonal variability, and the HLNP has the most significant heave trend. By fitting the mean heave timeseries in each region to our linear model at many depths, we can better understand the regional variability of natural and climatic changes in the North Pacific Ocean.

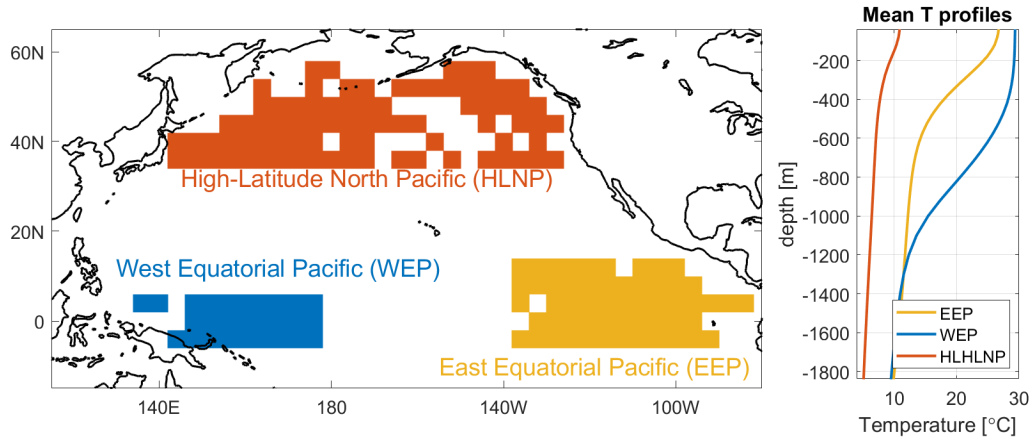

Figure 5.8: [Left] The three regions chosen for examining the linear model of heave. [Right] Mean temperature profile for each region. Colors correspond to like regions in both plots, for the East Equatorial Pacific (EEP, yellow), West Equatorial Pacific (EWP, blue), and the High-Latitude North Pacific (HLNP, orange). Gaps in spatial coverage are due to some locations being excluded for not having enough Argo data or having too many temporal gaps.

The model fit in the EEP is high overall, though the fit gradually decreases with depth (Fig. 5.9). ENSO is the strongest contributor to heave in the EEP, especially in the upper 750m of the ocean. Below 700m depth, the heave in the EEP is explained mostly by seasonal variability. The sign of the association between heave and the seasonal cycle reverses around 500m depth, which could be related to propagating equatorial waves that are out of phase with the seasonal cycle. Heave trends are not very significant in the EEP.

In the WEP, the model has a poor fit in the surface ocean, but the fit increases with depth (Fig. 5.9). There may be a process that greatly influences the surface ocean in the WEP that is not accounted for in the model. Seasonal variability has the strongest presence in heave in this region, especially below 1000m depth. Comparing the seasonal and ENSO variability in the WEP with the EEP reveals a sort of dipole structure between the two regions, which likely corresponds to how the two regions are coherent but often experience variability in opposite phases. Heave trends in the WEP also do not seem to be significant compared to ENSO and seasonal variability.

The structure of heave in the HLNP differs from the heave in the equatorial regions in several ways. Firstly, the HLNP has the best model fit at the surface, which is by seasonal variability and perhaps a small heave trend. Below 200m depth, heave variability in the HLNP is small compared to the EEP and WEP;

ENSO has a small contribution to heave in the HLNP, but mostly above 500m depth. Seasonal variability in the HLNP is more prominent than ENSO but also decays with depth. However, heave trends explain over half of the heave variability in the HLNP below 750m depth, and the model fit increases at the depths where the heave trend is present. The prominent heave trend in this region may be due to the low stratification in the HLNP compared to the Equatorial Pacific (Fig. 5.8), which allows for easier vertical heat exchange.

We thus expect the Equatorial Pacific to be primarily influenced by natural variability, and the High-Latitude North Pacific to be influenced by long-term heaving trends associated with ocean heat uptake. These regional variations are likely present all over the North Pacific and in other ocean basins; regional heave analysis is therefore useful for gaining a more complete understanding of ocean variability.

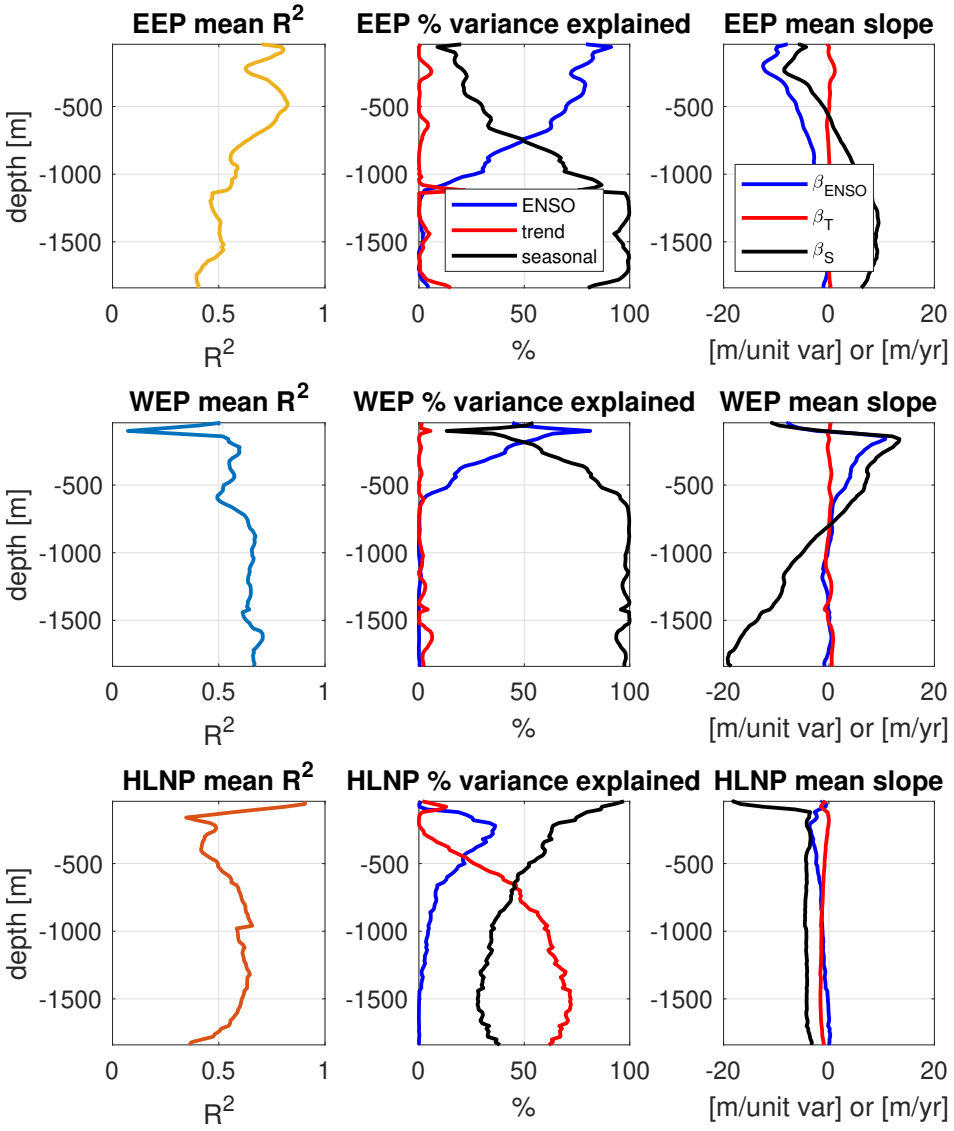

Figure 5.9: Depth-dependent linear model results for the mean heave timeseries from three regions: the East Equatorial Pacific (EEP, top row), West Equatorial Pacific (WEP, middle row), and the High-Latitude North Pacific (HLNP, bottom row). [Left] Model R^2, where higher values indicate better model fit. [Center] Percent of the heave variance explained by each model component, ENSO (blue), trend (red), and the seasonal cycle (black). Higher percentages indicate higher contribution to heave relative to the other components of the model. [Right] Slope associated with each model component. ENSO (blue) and seasonal (black) components are in units of m heave/unit variance, while the trend (red) is in units of m heave/year.

5.3.4 High-Latitude Heat Uptake

Out of the three regions we selected to study in detail, the high-latitude North Pacific experiences the most significant heave trend. We therefore decide to calculate the heat uptake in the high-latitude North Pacific. Ignoring the influence of salinity and pressure on heat content, we approximate the change in heat content Q as

$$\frac{dQ}{dt} = \left(\rho \cdot C \cdot \frac{dT}{dd}\right) \cdot \frac{dd}{dt}$$

where ρ is the density of seawater (we used 1029 kg m^{-3}), C is the specific heat of seawater (3850 J kg^{-1} C^{-1}), $\frac{dT}{dd}$ is the change in temperature per unit depth, and $\frac{dd}{dt}$ is the heave trend that we calculated for many locations and depths in our linear model (β_T). We calculate $\frac{dT}{dd}$ for each depth interval using the mean temperature profile in the high-latitude North Pacific, and the mean $\frac{dd}{dt}$ across the region for each depth interval. This yields a mean change in heat content at every depth in J yr^{-1} (Fig. 5.10).

We then integrate the heat content change across all depths and convert it to total heat uptake, which we find to be 0.88 W m^{-2}. 41% of this heat uptake occurs in the upper 200m of the high-latitude North Pacific, while the remaining 59% occurs from 200-1800m depth. This heat uptake estimate is on the same order of magnitude as previous estimates of heat uptake in the upper 2000m of the Pacific Ocean (*Roemmich et al.*, 2015; *Desbruyères et al.*, 2017).

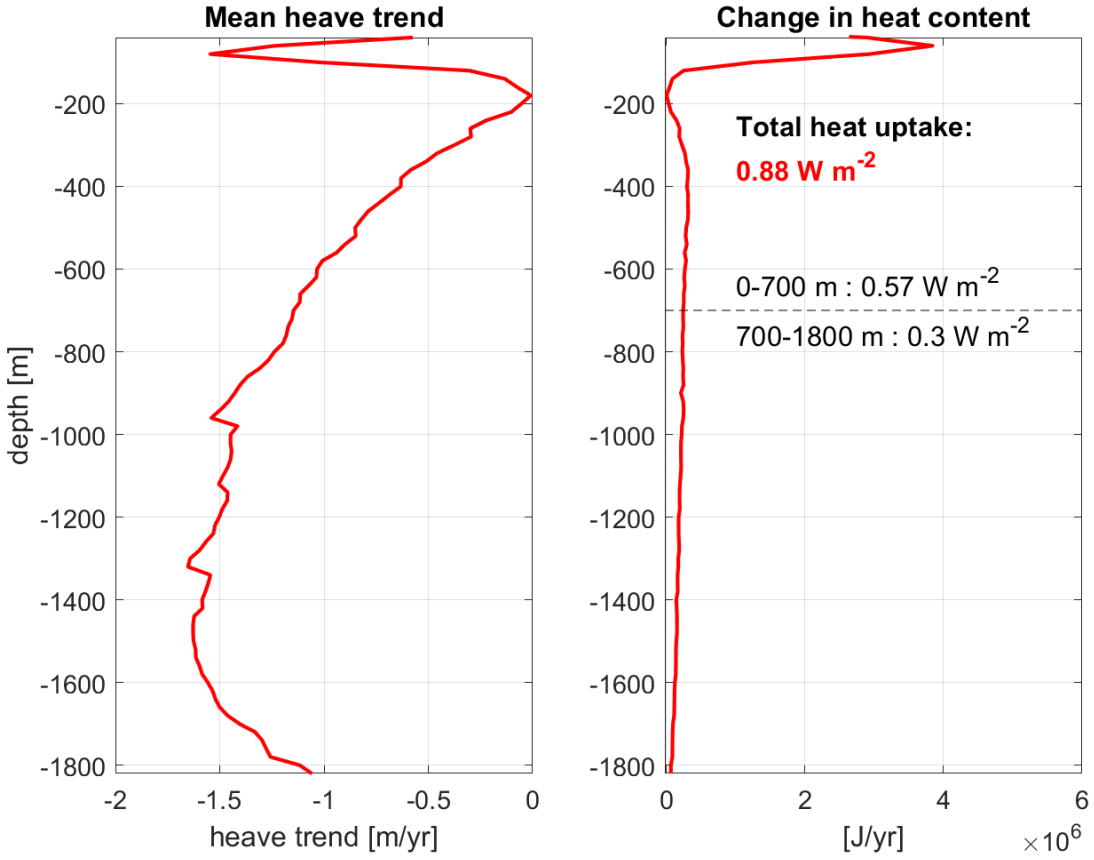

Figure 5.10: [Left] The heave trend (β_T) and [Right] the change in heat content averaged across the high-latitude North Pacific region as a function of depth. Change in heat content integrated with depth to yield heat uptake in the upper ocean (0-700m) and intermediate ocean (700-1800m).

5.4 Discussion

Using our novel method for calculating heave, Dual-Dynamic Depth Warping, we successfully converted the Argo data in the North Pacific into a format where we could observe natural and climatic influences on the ocean. Using a linear model and coherence analysis, we detected large-scale natural variability in the heaving of isopycnals associated with ENSO and seasonal changes. We identified regional variability, such as coherent wave patterns in the deep Equatorial Pacific. We were also able to use heave to describe the

seasonal cycle, ENSO relationship, and gradual northward migration of the Kuroshio Current. Finally, we quantified long-term heaving trends in the high-latitude North Pacific, converted these heaving trends to heat uptake, and detected positive heat uptake in the upper 2000m of the high-latitude North Pacific.

These results demonstrate the importance of quantifying regional variations in how natural and climatic processes influence ocean observations. This analysis shows potential to model how various atmospheric and oceanic processes contribute to heave, on the scale of individual currents to entire ocean basins. Although our simple heave model did not account for every source of heave variability in the North Pacific, and there was some indication that is missed an important surface process in the West Equatorial Pacific, this model was a good first step in partitioning heave into contributions from natural and climatic processes. This model allowed us to study relatively complex heave structures at many locations and depths in the North Pacific.

Future work should examine additional types of variability that are likely to influence heave in the North Pacific, as well as the spatial variability of ocean heat uptake. Using Argo data with higher depth resolution would also be helpful for capturing the full structure of heave in Argo, especially from 1000-2000m depth. The Argo product we used had a depth resolution of 100m below 1000m depth, which we interpolated to 4m depth resolution; this likely reduced the amount of heave variability we were able to detect. Higher-resolution Argo data at depth could be especially useful for studying equatorial waves.

Another logical next step would be to apply this analysis to the global Argo dataset, to study the structure of climatic and natural variability in the global ocean. However, there may be some obstacles to extending this analysis to other ocean basins. For example, basins with complex topography could influence heave signals and obscure dynamical changes in heave. Regions that frequently experience horizontal advection also pose problems for vertical heave analysis, though we hope to eventually improve our Dual-Dynamic Depth Warping technique to account for horizontal heave. These potential issues should be considered when implementing this analysis across the global ocean.

The greatest limitation in this Argo heave analysis is that the global Argo data do not measure the deep ocean. While calculating heat uptake in the upper 2000m of the ocean is useful, deep ocean data is needed to quantify ocean heat uptake and predict future consequences (*Li et al.*, 2013). This is an important reason to support the establishment of a global deep-Argo array. Until then, however, we can compare these Argo

results to other datasets, such as the TAO array and ship-based measurements. This could potentially help us extrapolate the variability of heave from the bottom of the Argo depth range into the deep ocean.

Chapter 6

Conclusions and Future Directions

This work presented a new method for measuring isopycnal heave called Dual-Dynamic Depth Warping, which used temperature and salinity measurements rather than the conventional use of potential density to quantify changes in the ocean. This novel method for calculating heave outperformed the conventional density-based methods in synthetic tests, especially for vertical profiles with low stratification and noise. Dual-Dynamic Depth Warping could also distinguish between vertical heave and horizontal advection, whereas density-based methods for calculating heave often mischaracterized lateral water mass intrusions as vertical heave or missed the change altogether.

Future work will test Dual-Dynamic Depth Warping further with different ocean profiles and optimize the weighting between temperature and salinity to measure heave accurately in a variety of stratifications. We also plan to adapt Dual-Dynamic Depth Warping to calculate heave in three dimensions. Treating heave as a three-dimensional process would not only allow us to quantify heave in regions with significant lateral advection, but it would also provide a more complete description of ocean variability.

However, Dual-Dynamic Depth Warping has already shown several advantages over conventional methods for calculating vertical ocean changes. This novel method has great potential to transform existing ocean datasets into a form that reveals more about the workings of the interior ocean than has been previously detected. We used Dual-Dynamic Depth Warping to characterize heave in station data from Hawaii and Bermuda, and found teleconnections to global climatic processes and evidence of seasonal and interannual variability in the deep ocean. These results align with previous findings about deep-ocean variability, and demonstrate the capacity of the deep ocean to respond to short-term changes. Resolving these short- and long-term changes in the deep ocean is critical for quantifying ocean heat content.

This work also provided the first Hawaii Ocean Timeseries/Argo comparison, where we found agreement

between heave estimates in the two datasets. This correspondence indicated that our analysis could be applied to the Argo dataset, thus expanding the potential scope of our analysis to the global ocean. Our results from using heave to measure natural and climatic changes in the North Pacific Argo data were promising. Using a simple linear model, we distinguished heave trends from seasonal and El Niño-related variability, and converted these heave trends to ocean heat uptake.

Future work should continue using heave trends to quantify ocean heat uptake in the Argo data, and explore nonlinear trends in ocean heat content. We recommend using both coherence analysis and a linear model to study ocean variability, especially in regions known to have coherent wave patterns, such as the Equatorial Pacific. Extending our analysis to Argo data in other ocean basins may be challenging due to variations in topography and horizontal advection, but comparing heave estimates in Argo to other datasets such as stations and ship-based measurements could help us verify our Argo heave estimates, as we did with the Hawaii station in this study.

The ultimate goal of this work is to develop a global climatology of heave, to understand how climatic and natural processes influence ocean observations in all regions of the world. Constraining heave and identifying the processes that cause heave allow us to not only observe how the ocean is changing, but also understand the drivers of variability in every corner of the ocean. Quantifying vertical heave in the North Pacific Argo data was a first step in this process. We plan to extend our analysis to the existing global Argo dataset. The frequent monitoring of the interior ocean provided by Argo has been shown to be crucial for quantifying both natural and climatic changes in the ocean, and our understanding of interior ocean variability will only improve with the expansion of the Deep-Argo program. Understanding the interior ocean in this much detail gives us more power to study changes in ocean circulation, constrain ocean heat content, and predict the broader impacts of ocean heat uptake in this warming climate.

References

(2016), Application Note 82: Guide to Specifying a CTD - Understanding Impacts on Accuracy.

Argo (2000), Argo float data and metadata from Global Data Assembly Centre (Argo GDAC), doi:10.17882/42182, type: dataset.

Berndt, D. J., and J. Clifford (1994), Using Dynamic Time Warping to Find Patterns in Time Series, *KDD Workshop*, *10*(16), 359–370.

Bindoff, N. L., and T. J. McDougall (1994), Diagnosing Climate Change and Ocean Ventilation Using Hydrographic Data, *Journal of Physical Oceanography*, *24*(6), 1137–1152, doi:10.1175/1520-0485(1994)024⟨1137:DCCAOV⟩2.0.CO;2.

Bryden, H. L., E. L. McDonagh, and B. A. King (2003), Changes in ocean water mass properties: Oscillations or trends?, *Science; Washington*, *300*(5628), 2086–8.

Church, J. A., N. J. White, L. F. Konikow, C. M. Domingues, J. G. Cogley, E. Rignot, J. M. Gregory, M. R. v. d. Broeke, A. J. Monaghan, and I. Velicogna (2011), Revisiting the Earth's sea-level and energy budgets from 1961 to 2008, *Geophysical Research Letters*, *38*(18), doi:10.1029/2011GL048794.

Desbruyères, D., E. L. McDonagh, B. A. King, and V. Thierry (2017), Global and Full-Depth Ocean Temperature Trends during the Early Twenty-First Century from Argo and Repeat Hydrography, *Journal of Climate*, *30*(6), 1985–1997, doi:10.1175/JCLI-D-16-0396.1.

Desbruyères, D. G., S. G. Purkey, E. L. McDonagh, G. C. Johnson, and B. A. King (2016), Deep and abyssal ocean warming from 35 years of repeat hydrography, *Geophysical Research Letters*, *43*(19), 10,356–10,365, doi:10.1002/2016GL070413.

Durack, P., P. Gleckler, S. Purkey, G. Johnson, J. Lyman, and T. Boywe (2018), Ocean Warming: From the Surface to the Deep in Observations and Models, *Oceanography*, *31*(2), 41–51, doi:10.5670/oceanog.2018.227.

Durack, P. J., and S. E. Wijffels (2010), Fifty-Year Trends in Global Ocean Salinities and Their Relationship to Broad-Scale Warming, *Journal of Climate*, *23*(16), 4342–4362, doi:10.1175/2010JCLI3377.1.

Forget, G. (2016), ECCO version 4 release 2: in situ and estimated profile data (MITprof data sets), doi:10.7910/DVN/EE3C40, type: dataset.

Forget, G., J.-M. Campin, P. Heimbach, C. N. Hill, R. M. Ponte, and C. Wunsch (2015), ECCO version 4: an integrated framework for non-linear inverse modeling and global ocean state estimation, *Geoscientific Model Development*, *8*(10), 3071–3104, doi:10.5194/gmd-8-3071-2015.

Gille, S. T. (2008), Decadal-Scale Temperature Trends in the Southern Hemisphere Ocean, *Journal of Climate*, *21*(18), 4749–4765, doi:10.1175/2008JCLI2131.1.

Häkkinen, S., P. B. Rhines, and D. L. Worthen (2016), Warming of the Global Ocean: Spatial Structure and Water-Mass Trends, *Journal of Climate*, *29*(13), 4949–4963, doi:10.1175/JCLI-D-15-0607.1.

Jayne, S., D. Roemmich, N. Zilberman, S. Riser, K. Johnson, G. Johnson, and S. Piotrowicz (2017), The Argo Program: Present and Future, *Oceanography*, *30*(2), 18–28, doi:10.5670/oceanog.2017.213.

Jayne, S. R., and J. Marotzke (2001), The dynamics of ocean heat transport variability, *Reviews of Geophysics*, *39*(3), 385–411, doi:10.1029/2000RG000084.

Johnson, G. C., J. M. Lyman, and S. G. Purkey (2015), Informing Deep Argo Array Design Using Argo and Full-Depth Hydrographic Section Data, *Journal of Atmospheric and Oceanic Technology*, *32*(11), 2187–2198, doi:10.1175/JTECH-D-15-0139.1.

Johnson, H. L., and D. P. Marshall (2002), Localization of abrupt change in the North Atlantic thermohaline circulation, *Geophysical Research Letters*, *29*(6), 7–1–7–4, doi:10.1029/2001GL014140.

Karl, D. M., and R. Lukas (1996), The Hawaii Ocean Time-series (HOT) program: Background, rationale and field implementation, *Deep Sea Research Part II: Topical Studies in Oceanography*, *43*(2), 129–156, doi:10.1016/0967-0645(96)00005-7.

Katsumata, K. (2016), Eddies Observed by Argo Floats. Part I: Eddy Transport in the Upper 1000 dbar, *Journal of Physical Oceanography*, *46*(11), 3471–3486, doi:10.1175/JPO-D-16-0150.1.

Kawase, M. (1987), Establishment of Deep Ocean Circulation Driven by Deep-Water Production, *Journal of Physical Oceanography*, *17*(12), 2294–2317, doi:10.1175/1520-0485(1987)017⟨2294:EODOCD⟩2.0.CO;2.

Li, C., J.-S. von Storch, and J. Marotzke (2013), Deep-ocean heat uptake and equilibrium climate response, *Climate Dynamics*, *40*(5-6), 1071–1086, doi:10.1007/s00382-012-1350-z.

Lukas, R., and F. Santiago-Mandujano (1996), Interannual variability of Pacific deep- and bottom-waters observed in the Hawaii Ocean Time-series, *Deep Sea Research Part II: Topical Studies in Oceanography*, *43*(2), 243–255, doi:10.1016/0967-0645(95)00103-4.

McDonagh, E. L., H. L. Bryden, B. A. King, R. J. Sanders, S. A. Cunningham, and R. Marsh (2005), Decadal Changes in the South Indian Ocean Thermocline, *Journal of Climate*, *18*(10), 1575–1590, doi:10.1175/JCLI3350.1.

McDougall, T. J. (1984), The Relative Roles of Diapycnal and Isopycnal Mixing on Subsurface Water Mass Conversion, *Journal of Physical Oceanography*, *14*(10), 1577–1589, doi:10.1175/1520-0485(1984)014⟨1577:TRRODA⟩2.0.CO;2.

McDougall, T. J., and P. C. McIntosh (2001), The Temporal-Residual-Mean Velocity. Part II: Isopycnal Interpretation and the Tracer and Momentum Equations, *Journal of Physical Oceanography*, *31*(5), 1222–1246, doi:10.1175/1520-0485(2001)031⟨1222:TTRMVP⟩2.0.CO;2.

Michaels, A. F., and A. H. Knap (1996), Overview of the U.S. JGOFS Bermuda Atlantic Time-series Study and the Hydrostation S program, *Deep Sea Research Part II: Topical Studies in Oceanography*, *43*(2), 157–198, doi:10.1016/0967-0645(96)00004-5.

Mitchum, G. T. (1996), On using satellite altimetric heights to provide a spatial context for the Hawaii Ocean Time-series measurements, *Deep Sea Research Part II: Topical Studies in Oceanography*, *43*(2), 257–280, doi:10.1016/0967-0645(95)00091-7.

Nerem, R. S., B. J. Haines, J. Hendricks, J. F. Minster, G. T. Mitchum, and W. B. White (1997), Improved determination of global mean sea level variations using TOPEX/POSEIDON altimeter data, *Geophysical Research Letters*, *24*(11), 1331–1334, doi:10.1029/97GL01288.

Nieves, D., and M. Spall (2018), Propagation of North Atlantic Deep Water Anomalies, *Journal of Physical Oceanography*, *48*(8), 1831–1848, doi:10.1175/JPO-D-18-0068.1.

Palmer, M. D., D. J. McNeall, and N. J. Dunstone (2011), Importance of the deep ocean for estimating decadal changes in Earth's radiation balance, *Geophysical Research Letters*, *38*(13), doi:10.1029/2011GL047835.

Purkey, S. G., and G. C. Johnson (2010), Warming of Global Abyssal and Deep Southern Ocean Waters between the 1990s and 2000s: Contributions to Global Heat and Sea Level Rise Budgets*, *Journal of Climate*, *23*(23), 6336–6351, doi:10.1175/2010JCLI3682.1.

Purkey, S. G., and G. C. Johnson (2013), Antarctic Bottom Water Warming and Freshening: Contributions to Sea Level Rise, Ocean Freshwater Budgets, and Global Heat Gain, *Journal of Climate*, *26*(16), 6105–6122, doi:10.1175/JCLI-D-12-00834.1.

Qiu, B., and R. Lukas (1996), Seasonal and interannual variability of the North Equatorial Current, the Mindanao Current, and the Kuroshio along the Pacific western boundary, *Journal of Geophysical Research: Oceans*, *101*(C5), 12,315–12,330, doi:10.1029/95JC03204.

Rayner, N. A., D. E. Parker, E. B. Horton, C. K. Folland, L. V. Alexander, D. P. Rowell, E. C. Kent, and A. Kaplan (2003), Global analyses of sea surface temperature, sea ice, and night marine air temperature since the late nineteenth century, *Journal of Geophysical Research: Atmospheres*, *108*(D14), doi:10.1029/2002JD002670.

Reid, J. L. (1997), On the total geostrophic circulation of the pacific ocean: flow patterns, tracers, and transports, *Progress in Oceanography*, *39*(4), 263–352, doi:10.1016/S0079-6611(97)00012-8.

Rhein, M., S. Rintoul, S. Aoki, E. Campos, D. Chambers, R. Feely, S. Gulev, G. Johnson, S. Josey, A. Kostianoy, C. Mauritzen, D. Roemmich, L. Talley, and F. Wang (2013), Observations: Ocean, in *Climate Change 2013: The Physical Science Basis. Contribution of Working Group I to the Fifth Assessment Report of the Intergovernmental Panel on Climate Change*, edited by T. Stocker, D. Qin, G.-K. Plattner, M. Tignor, S. Allen, J. Boschung, A. Nauels, Y. Xia, V. Bex, and P. Midgley, pp. 255–316, Cambridge University Press, Cambridge, United Kingdom and New York, NY, USA, doi:10.1017/CBO9781107415324.010.

Roemmich, D., G. Johnson, S. Riser, R. Davis, J. Gilson, W. B. Owens, S. Garzoli, C. Schmid, and M. Ignaszewski (2009), The Argo Program: Observing the Global Oceans with Profiling Floats, *Oceanography*, *22*(2), 34–43, doi:10.5670/oceanog.2009.36.

Roemmich, D., J. Church, J. Gilson, D. Monselesan, P. Sutton, and S. Wijffels (2015), Unabated planetary warming and its ocean structure since 2006, *Nature Climate Change*, *5*(3), 240–245, doi:10.1038/nclimate2513.

Schmitt, R. (2018), The Ocean's Role in Climate, *Oceanography*, *31*(2), doi:10.5670/oceanog.2018.225.

Wijffels, S., D. Roemmich, D. Monselesan, J. Church, and J. Gilson (2016), Ocean temperatures chronicle the ongoing warming of Earth, *Nature Climate Change*, *6*(2), 116–118, doi:10.1038/nclimate2924.